# Validation of a Xenobiotic Vapor Generation and Exposure Chamber System for Quantification of Exposure Effect in 3-Dimensional Human Tissue Reconstructs

By

Kennedy M. Holt

A technical report submitted to the faculty of the University of North Carolina at Chapel Hill in partial fulfillment of the requirements of the degree of Master of Science in Public Health in the Department of Environmental Sciences and Engineering

Chapel Hill

2014

**Approved By:**

Advisor: Dr. Leena A. Nylander-French

Reader: Dr. Ken Sexton

Reader: Dr. Michael Flynn

**Abstract**

As the number of manufactured xenobiotics continues to increase, the need for accurate, reproducible methods for quantifying exposure and the related health effects becomes more imperative. My Master Thesis goal was twofold: (1) develop an exposure-chamber system capable of delivering a constant concentration of a xenobiotic vapor and (2) quantify the effect of benzene (as a model xenobiotic) vapor exposure using commercial *in vitro* 3-dimentional (3D) human skin and lung tissue reconstructs. These reconstructs were exposed to clean air, 30 ppm, 60 ppm, or 120 ppm of benzene for 6 h per day for 5 consecutive days. The concentration of benzene in the exposure-generation system was measured in real-time using gas chromatography-flame ionization detection. Cytotoxicity was determined in the tissue culture media using spectrophotometry. Morphological changes in the tissue reconstructs were observed through histological staining using both hematoxylin and eosin as well as Periodic acid–Schiff stains. The results demonstrate that the exposure-chamber system can deliver a constant concentration of benzene vapor for an extended period of time. The skin reconstructs showed no evidence of toxicity at the levels ≤120 ppm while the lung reconstructs indicated a potential dose-response to benzene exposure. The absence of toxicity in the skin reconstructs indicates that the stratum corneum serves as an effective protective barrier towards benzene vapor exposure. The observed responses in the lung reconstructs provide evidence that this model is amenable for biological assessment of toxic effects due to xenobiotic vapor exposure. This research provides a foundation to further develop methods using 3D human reconstruct models for evaluation of adverse effects due to xenobiotic exposure.

# Table of Contents

# List of Figures

# List of Tables

# List of Abbreviations

| | |
|---|---|
| 2D | two-dimensional |
| 3D | three-dimensional |
| ACGIH | American Conference of Governmental Industrial Hygienists |
| ADME | absorbed, distributed, metabolized, and eliminated |
| FID | flame-ionization detector |
| GC | gas chromatograph |
| GC-MS | gas chromatography-mass spectrometry |
| H&E | hematoxylin and eosin |
| IARC | International Agency for Research on Cancer |
| IRB | institutional review board |
| LDH | lactate dehydrogenase |
| NHBE | normal human tracheal/bronchial epithelial cells |
| NHDF | normal human fibroblasts |
| NHEK | normal human keratinocytes |
| NTP | National Toxicology Program |
| PAS | Periodic acid-Schiff |
| PBS | phosphate buffered saline |
| PID | photo-ionization detector |
| ppb | parts per billion |
| ppm | parts per million |

# INTRODUCTION

## 1.1 Background

Biologically relevant methods for measuring human exposure to air toxics and their health effects are urgently needed. The recent report from the National Academy of Sciences, Toxicity Testing in the 21st Century, is a roadmap for the development of predictive *in vitro* and *in vivo* models for exposure assessment and biological response to be used in human risk assessment (NRC, 2007). To this end, progress has been made using two-dimensional (2D) monolayer and three-dimensional (3D) cell-culture models to learn about health effects of exposures as they would occur *in vivo* (Liu *et al.*, 2013). These advances are limited in that they can only show what happens within single cells and not in whole tissues. To overcome these shortcomings, several exposure models have been developed to provide conditions that closely mimic native human exposure conditions as they occur *in vivo*.

Significant advances can be made through the development of methods to measure exposure to air toxics and resultant toxic events using *in vitro* human 3D organotypic tissues (*i.e.*, reconstructs) (Pampaloni, 2007). To spur these advances, we have developed an *in vitro* air-monitoring device that can be utilized to perform controlled *in vitro* exposures to air toxics in simulated exposure conditions to mimic repeated exposure scenarios as is common in both environmental and occupational exposure situations. Our exposure system allows for simultaneous delivery and quantitation of a specific concentration of the desired air toxin to the *in vitro* cell or tissue culture system for assessment of biological response to air toxic exposure.

Since initial exposure to air toxics usually involves lung and skin, 3D reconstructs of these tissues served as our models to test the efficacy of the developed exposure-chamber system. We

utilized *in vitro* 3D human lung and skin tissue reconstructs to detect and measure the toxicity of benzene vapor, a volatile ubiquitous human carcinogen (Rappaport *et al.*, 2013). We hypothesized that our novel air-monitoring and benzene delivery system can be used to correlate benzene exposure with a dose-related toxicological response (*i.e.*, cytotoxicity, genotoxicity, and inflammatory cytokine expression) in the 3D human lung and skin reconstructs. After we have successfully tested and validated this device in the laboratory conditions, we can proceed to testing and validation for field use. In addition, this device has a potential to become an important tool for biomarker discovery, contribute to understanding of exposure dose-effects relationships, and ultimately, advance the science of human exposure and risk assessment.

## 1.2 Air Toxics Monitoring

Monitoring of air toxics is generally performed using direct-reading instruments or laboratory analysis of air samples obtained through various collection methods. While both methods are viable, neither provides the information necessary to rapidly screen for both the toxicity and concentration of airborne contaminants. These disadvantages stress the importance of developing specific, sensitive, and rapid methods for monitoring air toxics (Harper, 2000).

### *1.2.1 Sorbents*

The use of sorbents has been one of the most common methods to monitor air toxics since being implemented in the 60's. The use of sorbents allows for an atmospheric "snapshot" to be collected and then later analyzed in the laboratory for contaminants and their concentrations. Over the years as the number of known air toxics has increased, the need for a variety of sorbents and techniques that allow us to measure these air toxics in the environment has also increased. This, in turn, has

necessitated the development of porous polymers, carbon sieves, and thermal desorption techniques among other advances (Harper, 2000; Woolfenden, 2010).

While providing valuable information about the type and the magnitude of exposure to air toxics, sorbent techniques do not allow for real-time, rapid detection of air toxics. Each sorbent, after air sampling, must be taken to the laboratory for processing and chemical analysis in order to determine the type and extent of exposure in the sampled environment. Additionally, sorbent techniques are limited in specificity and sensitivity by the type of sorbent and/or the solvent used to wash the sorbent (Harper, 2000). These limitations present a problem if the exposure is unknown because choosing the most appropriate sorbent and/or solvent for an unknown air toxic would be difficult.

### *1.2.2 Direct-reading Instruments*

Direct-reading instruments have been used as early warning devices for monitoring air toxics in industrial settings where accidents and leaks could lead to high and/or toxic concentrations of a chemical(s) in the environment. These measurements are commonly carried out with the use of flame-ionization and photo-ionization detectors (FIDs and PIDs, respectively) (Krol *et al.*, 2010). Other instruments for real-time detection are also available, such as infrared spectrometry, but they are more cumbersome to use and require significant knowledge on the instrumentation (Green *et al.*, 1993). FID and PID devices are useful in occupational environments with known exposures because of the ease of mobility and the real-time feedback they provide of the concentration and concentration changes over time. These mobile air-toxic detection devices are often designed to detect only one single air toxic at any given time. This allows for a greater sensitivity, down to parts per million (ppm), for the selected contaminant along with rapid detection and analysis. Adversely, this type of detector is unable to provide accurate quantitative data in the presence of

multiple air toxics. However, the availability of mobile gas-chromatography mass-spectrometry (GC-MS) systems has facilitated the use of direct-reading instruments in the presence of multiple air toxics (Krol *et al.*, 2010).

Without the use of a mobile MS-GC direct-reading device, the use of other sampling methods is needed in order to determine exposure concentrations in the presence of multiple air toxics due to potential interference of xenobiotics with similar chemical and physical properties. Coupling the use of sorbent method with a direct-reading instrument can provide a greater understanding of the overall exposure situation. However, these detection methods do not provide information relating the exposure to human health effects. Furthermore, these monitoring methods have to be tailored for each contaminant measured and, therefore, the time needed to gather exposure information increases considerably. The lengthy amount of time between exposure analyses, along with the lack of exposure-effect data, has spurred the need for the development of rapid, real-time monitoring methods that quickly quantify and identify exposures and the potential adverse effects on humans (Molhave, 1997; Harper, 2000).

## 1.3 Models for Assessing the Biological Response of Air Toxics

The biological responses for air toxics is generally determined in experimental animal, *in vitro* cultured primary cell or transformed cell line, *in vitro* 3D tissue reconstruct, or human volunteers studies. The use of one or more of these models for exposure-effect studies allows us to determine the potential human response to air toxics exposure.

### *1.3.1 Animal Models*

When attempting to rapidly screen for airborne xenobiotics, animal models have varying degrees of effectiveness. The structure, organization, and function of animal systems may differ greatly

from that of humans, which could result in exposure and biological responses different from those that occur in humans (Tupker 2003). These species-specific variations are readily apparent in one of the most commonly used animal models, mice. Mouse lung and skin are significantly different from human lung and skin in its architecture and varies in response to xenobiotic exposure (Chillcott, R.T., 2008). The epidermis of mice is much thinner compared to human skin, measuring at a third of the thickness of the human epidermis. The diminished barrier function of the mouse skin creates a significant change in the functionality of the two skin types potentially altering exposure-effect relationships (Poet and McDougal, 2002). Highlighting these differences, mice exhibit a greater sensitivity to benzene exposures than humans, which can be attributed to differences in how benzene is absorbed, distributed, metabolized, and eliminated (ADME) in the two species (Henderson, 1996). However, animal models can be manipulated to express or inhibit known human factors of toxicity to benzene (Cliona *et al.*, 2011). For example, the use of CYP2E1 knockout mice helped determine that benzene-induced cytotoxicity was inhibited without CYP2E1 proteins (Valentine *et al.*, 1996). Similar studies using animal models allow us to predict or extrapolate how various factors could affect human exposure-effect responses.

Despite the potential shortcomings of animal models, they do present a unique opportunity to observe whole-system health effects due to air toxic exposure (McDougal, 1985; Morgan, 1991). Whereas both *in vitro* cell and tissue models can only provide an indication of how an exposure affects a specific, isolated part of a system. However, animal studies can be expensive, thus, limiting the extent to which animal models can be used to discern the effects multiple air-toxics exposures.

### *1.3.2 2D Monolayer Cell Cultures*

The biological activity of xenobiotics is commonly investigated using 2D monolayer cell cultures. These cell culture systems have become an invaluable tool for determining toxic responses that can be potentially triggered as a result of exposure to air toxics. Commercially available cells and cell lines can be used without an institutional review board (IRB) approval and, thus, these model systems are readily available for a multitude of toxicity studies, including for testing xenobiotics. A number of well-known cell models exists, each of which have advantages and disadvantages. Transformed cell lines have an unlimited lifespan allowing prolonged studies, but may not exhibit *in vivo-like* cell responses because the genotype and phenotype of transformed cells differ from that of normal cells (Foster *et al.*, 2000). Primary human cells, however, may provide a more realistic exposure response but are more challenging to isolate and culture from human tissues (Schwarze *et al.*, 1996). However, the limited lifespan and variability in response of primary cells may weaken the statistical associations and the power of a study (Brohem *et al.*, 2010 & Schaffer et al. 2014). In monocultures, the lack of other cell types can cause exposure effect relationships that are altered from observed exposure effect relationships observed in humans, as they may lack expression of the requisite biotransformation enzymes (Castell *et al.*, 2005). Similarly, cell lines may show altered expression of a range of secretory and signaling molecules that could alter growth and death patterns in the cells (Forbes & Ehrhardt, 2005). Gene expression profiles do not provide complete mechanistic details of toxicity from an exposure, thus potentially omitting exposure effects exhibited in other systems due to changes in altered gene expression (Castel et al., 2005 & Forbes and Ehrhardt, 2005). Furthermore, cultured cells require a sterile growth environment and specific growth conditions that may restrict the ability to use cell lines in occupational exposure environments. Potentially, the environmental conditions required for 2D

cell models have been shown to trigger false positive and negative findings (Brohem *et al.*, 2010). These biased findings can be a result of differences in phenotype, cellular signaling, cell migration, and drug response that arise from the environmental culture conditions of the 2D cell models.

While 2D monolayer cell cultures provide insights into the cellular impact of an exposure, they do not provide a rapid method for determining the concentration of an exposure to a xenobiotic. For both primary cell and cell line models, the absence of other parts of the human system create an exposure response that does not account for intercellular interactions (Brohem *et al.*, 2010). However, the use of cell culture models allows for a greater sample size because of the lower cost and ease of working with this models (Murphy, 1991). The increased sample size enables us to test a wider range of xenobiotics and investigate a greater variety of health endpoints. However, the inherent biases of 2D cell models have led to the development of highly differentiated 3D cell-culture models that have more *in vivo*-like characteristics by enabling cell-cell interactions, differentiation, and tissue consistent maturation (Liu, 2013).

### *1.3.3 3D Human Tissue Models*

A number of *in vitro* human tissue models have been developed (*i.e.*, human cadaver tissues, human excised tissues, and human tissue reconstructs). *In vitro* human tissues offer a unique perspective for toxicology studies with airborne contaminants because the model mimics the cellular interactions that occur within normal human tissues. In the absence of *in vivo* studies, both *ex* vivo and *in vitro* tissue models present the best opportunity to observe how various tissues respond to xenobiotic exposures. *Ex vivo* models, while removed from the body, still exhibit the characteristics of a tissue *in vivo*. This allows for targeted xenobiotic exposures that elicit responses similar to those found in tissues *in vivo*. *In vitro* tissue models provide a similar analysis of xenobiotic exposure with the added benefit of decreased variability. *In vitro* human tissue models

can be reproduced using exact methods repeatedly. This reduces variability between samples and minimizes the number of factors that can interfere with an exposure response.

Human cadaver/excised tissues models are used for investigating exposure-effect outcomes *ex vivo*. These *ex vivo* models are similar to *in vitro* 3D tissue reconstruct models except that the tissues are obtained from human subjects. However, these tissues are hard to obtain and the variability in sample quality is an issue (Hu, 2010). The variability in these tissues is mostly related to differences in donor sites, gender, race, and sample preparation (Poet and McDougal, 2002). Another disadvantage to using *ex* vivo models is the limited lifespan (Gibbons et al, 2013), which greatly restricts the duration for the experiments. Similar to 2D cell culture models, false positive or false negative results may occur due to disease or genetics variations in human cadaver/excised tissues (Elliot and Yuan, 2010). In addition, the use of these tissue requires patient consent and an IRB approval for the study.

*In vitro* 3D human tissue reconstructs are developed to mimic actual human tissues as closely as possible (Milchak, 2013; Gwinn *et al.*, unpublished). The use of 3D tissue reconstructs ensures a more uniform and readily available sample pool because they are grown from primary cells, which are sufficiently available for laboratory research, following specific tissue culture protocols (Brohem *et al.*, 2010). This uniformity between tissues provides good reproducibility. In addition, there is a potential to engineer these reconstructs with specific genetic alterations to investigate the influence of genetic variability in exposure-effect outcomes (Brohem *et al.*, 2010). When compared to both *ex vivo* and animal models, *in vitro* tissue reconstructs offer a model that is less expensive and eliminates significant ethical concerns that burden animal and human studies (Gibbons *et al.*, 2013). Additionally, human tissue reconstructs offer a more feasible model to observe effects of airborne toxics in occupational settings because they are more resilient than cells

cultures to sub-optimal environmental conditions and easier to us in the work environment than animals (Brohem *et al.*, 2010).

Despite all of the advantages of the 3D human reconstruct system, this model does not perfectly reflect *in vivo* responses. The differences can arise from cell-culture media and culture conditions and anatomical differences (i.e. lack of sweat glands in skin reconstructs) that may influence the production of the reconstructs (Gibbs, 2007). 3D human tissue models have expressed metabolic pathways similar to those seen in *in vivo* tissues, but further research is need to define the similarities and differences between the *in* vitro and *in vivo* (Hu, 2010). The ability to rapidly produce uniform 3D human reconstruct tissues with metabolic similarities and to observe morphological changes has a potential to offer insight into previously unknown exposure-effect outcomes (Gibbons *et al.*, 2013).

### *1.3.4 Human Volunteers*

Human exposure studies provide the most human-specific data when investigating the potential health effects due to exposure to air toxics. Using an exposure chamber, a specific concentration of the desired exposure can be delivered to a subject and the exposure pathway can be controlled. For example, subject can be fitted with a supplied-air respirator if skin only exposure to air toxic is investigated separately from inhalation exposure. The atmospheric conditions of the chamber can be finely controlled, which eliminates possible interference due to variability in exposure level and/or other air toxics that could cause similar toxic response (Weisel, 2002).

The problem with human exposure studies, much like human tissue studies, comes from the inherent variability between subjects as well as safety and ethical considerations. Differences in human metabolism and genetics can induce significant variability in biological responses to

xenobiotic exposure (Murugesan, 2013). To offset this variability, a large sample population is required, which can be difficult to obtain and is expensive. Furthermore, research on humans requires IRB approval with extensive measures taken to ensure that subjects are safe and fully knowledgeable about the exposure and the potential consequences. These issues create huge barriers for performing exposure studies on air toxics with humans.

### 1.4 Benzene

Benzene is a common solvent used in the production of consumer products and a constituent in air pollution. The unwanted health effects associated with both skin and inhalation exposure to benzene has been documented (ATSDR, 2007). Typically, these exposures are via liquid and/or vapor exposures. Skin exposure to benzene can result in irritation and dermatitis at the area of contact. The acute health effects associated with the inhalation of benzene vapors include headaches, fatigue, and respiratory/cardiac arrest (Luttrell and Conley, 2011). The adverse health effects of chronic exposure to benzene has been reported in numerous studies (Bahadar *et al.*, 2014). As a result, benzene is classified as an A1 human carcinogen by the American Conference of Governmental Industrial Hygienists (ACGIH) with chronic exposure increasing the risk of leukemia (ACGIH 2011). The National Toxicology Program (NTP) lists benzene as a known human carcinogen and the International Agency for Research on Cancer (IARC) classifies benzene as Group 1 carcinogenic to humans (ATSDR, 2007).

Liquid benzene is rapidly absorbed and penetrates the skin and readily enters into the systemic circulation (Blank, 1985). Rapid skin absorption of liquid benzene through the skin suggests that benzene vapor could also rapidly penetrate the skin. Benzene vapor penetrates lung tissue rapidly, with less than 10% of the total inhaled benzene being expired over a 3 h exposure (Yu and Weisel, 1996). In a biological model system, benzene can elicit a cytotoxic response in

the release of lactate dehydrogenase (LDH) into the media, which can be easily measured using spectrophotometric methods (Pariselli *et al.*, 2009). Benzene is a ubiquitous environmental xenobiotic, which is rapidly absorbed through various human tissues and has known and measurable health effects. These characteristics make benzene an ideal xenobiotic for measuring the efficacy of our exposure mixture generation and chamber system.

### 1.5 The Goal of the Study

In this research project, I investigated the use of a real-time *in vitro* air-monitoring device for screening and quantification of air toxics exposure. I hypothesized that (1) a real-time exposure-generation system can deliver a constant flow and concentration of benzene to an *in vitro* exposure chamber and (2) *in vitro* 3D human skin and lung reconstructs can be used to quantify the toxicity of benzene. To test my hypotheses, I exposed 3D human skin and lung reconstructs to known concentrations of benzene using our exposure-chamber system and analyzed morphological and cytotoxic effects of the exposure. Both skin and lung reconstructs were used because they serve as different routes of exposure to air toxics and, therefore, may exhibit different exposure-effect outcomes. In addition, uniformity among the reconstructs and their similarities to *in vivo* tissues will provide the best means to determine an exposure-effect relationship. Validation of the exposure generation and the chamber system for *in vitro* exposure and toxicity assessment in the tissue reconstructs, will confirm the utility of this tool for use in quantification of exposure-effect relationships of air toxics *in vitro*.

## 2. Materials and Methods

### 2.1 Exposure-chamber System and Generation of Benzene Vapor

The *in vitro* lung and skin reconstructs were kept under constant relative humidity (~80%) at 37$^{o}$C with 5% $CO_2$ and exposed to a well-mixed and controlled continuous stream of either clean air or air containing benzene at the desired concentration as shown in the diagram in Figure 1. Two chambers were utilized for simultaneous tissue exposure to two different concentrations of benzene vapor or humidified clean air (as the control) (Figure 1).

The benzene vapor concentration was primarily controlled by the temperature of the diffusion tube (housed in a temperature adjustable chamber) via rate of evaporation and diffusion out of a small diameter tube. The benzene concentration was further adjusted by dilution with clean air and humidified by passing through an impinger containing water. We used the temperature settings of 42$^{o}$C for the 30 ppm and 60 ppm exposures and 53$^{o}$C for the 120 ppm exposure.

After placing the benzene diffusion tube within the temperature-controlled chamber (air mixture flow rate controlled by the rotameter), the system required two hours to equilibrate. This equilibration time was determined by monitoring the benzene concentration in the exposure chamber using a Varian CP-3800 gas chromatograph (GC) and recording the time when the exposure chamber concentration did not vary more than 1% between measurements. These measurements were taken every 30 min to ensure that the column was flushed in between samples.

The exposure generation system used clean air from a clean-air generator (Aadco 737 Pure Air Generator, Aadco Instruments, Cleves, OH) that removes any possible contaminants and is tested by conducting clean air sham exposures. The "zero air" from the 737-250 Pure Air Generator exceeds requirement for purity. AADCO's purity specifications are: <1 ppb ozone, methane,

hydrocarbons, NO/NOx, H2S, S02, COS, CO, CO2, SF6 and fluorocarbons. All particulates are removed from the source air and never appear in the air generated.

Clean air was used to dilute benzene vapor emitted from a diffusion tube to create a primary and constant concentration of benzene vapor. The resulting mixture was further diluted, as needed, with clean humidified air to achieve the target benzene concentration for in vitro exposures. This system uses multiple Aalborg GFC171 and GFC17 mass-flow controllers to pass air through heated impingers, in series, containing 15 mL HPLC grade water (submicron filtered, Lot 134926; Fisher Scientific, Waltham, MA) to humidify the air. The incorporation of humidified air prevented dehydration of the tissue reconstructs during the course of the 6-h exposure by maintaining a suitable relative humidity.

The initial source of benzene vapor was generated by slowly evaporating 2 mL of liquid benzene contained in a glass diffusion tube placed within a heated chamber. This chamber was regulated by a non-adjustable flow restrictor and monitored with a rotameter, which measures flow rate. A short piece of small diameter (0.25 in) Teflon™ tubing was inserted into the opening of the diffusion tube to limit and control the amount of benzene vapor leaving the tube (Nelson, 1971). Benzene vapor was then mixed in an internal flask using clean dilution air controlled with another valve and rotameter. Throughout the system, Teflon™ tubing (0.25in diameter) was used due to its inert properties in order to minimize exposure of reconstructs to potential chemical contaminants and prevent the loss of benzene due to tube-wall absorption. A separate line of clean air was humidified and then combined with benzene-laden air to create the benzene concentration for the first exposure chamber. An additional supply of clean, humidified air was connected later in the line to create a second benzene concentration which allowed for the simultaneous exposure of two benzene concentrations.

Each tissue exposure chamber consisted of a plastic clam shell with an elevated grate bottom on which to suspend the plate containing the reconstructs above the entry and exit points of the stream of air (modulator incubator chamber, Model #5352414; Billups-Rothenburg, Del Mar, CA). This allowed for the air to circulate around the reconstructs and ensured that each reconstruct received the same exposure as the others in the plate.

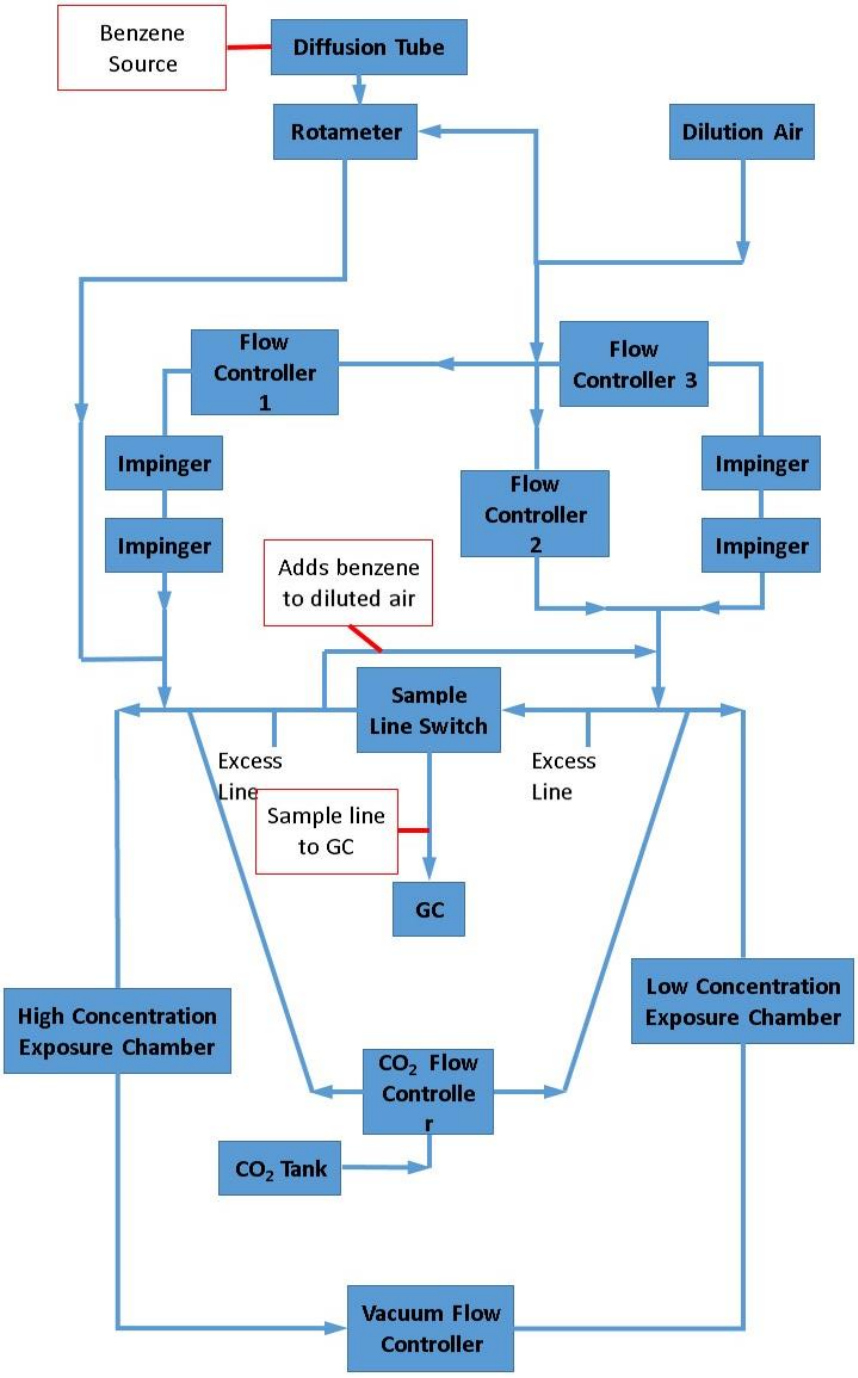


**Figure 1**. A diagram of the exposure chamber system used to perform the exposure experiments. The system starts on the top side of the diagram progressing down, following the arrows and lines to depict the direction of the airflow. The boxes depict different compartments that the air passes through with the lines depicting the sample lines connecting the compartments.

The benzene vapor concentration in the two chambers was continuously monitored using the GC to track the stability of the system. This was accomplished by switching the sample line between the two exposure chambers by use of a t-valve. Ten minutes prior to a sample injection in the GC, the sample line was switched to the other exposure chamber to clear the residual air out of the column. While simultaneous monitoring of both exposure chambers would have been preferable, we did not have the equipment to perform simultaneous monitoring.

**2.2 Tissue Reconstructs**

Commercial lung and skin constructs, EpiAirway Lung Tissues (AIR-606; MatTek, Ashland, MA) and EpiDerm Skin Tissues (EFT-306; MatTek) shown in Figure 2, were used to test our exposure system. These tissue reconstructs were chosen because of their similarity in structure to human tissues in vivo (Figure 3), the uniformity between each reconstruct, and the similarity in function they have in comparison to real human skin and lung tissues (Milchak, 2013; Gwinn *et al.*, unpublished).

Both the skin and lung reconstructs were grown in 6-well plates in a Millicell tissue culture insert (Millipore, MA, Billerica). Upon delivery, the reconstructs were separated into fresh 6-well plates with each exposure group occupying its own plate. All of the plates were placed inside a humidified cell-culture incubator maintained at 37$^{o}$C and 5% $CO_2$. Each day, the medium from the wells was replaced with fresh medium. The removed medium was saved frozen for later analysis. The skin and lung reconstructs were fed 1 mL of medium (EFT-300-ASY and AIR-100-ASY-PRF, respectively; MatTek). After media changes, the reconstructs were exposed to either clean air or benzene while the non-exposed reconstructs (*i.e.*, unexposed incubator control) were placed back into the cell-culture incubator.

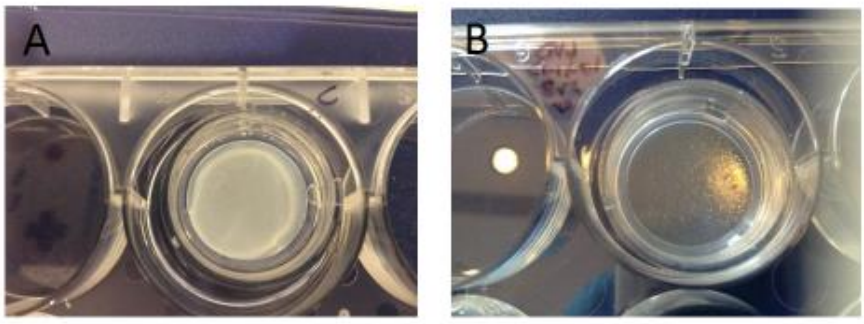


**Figure 2**. An EpiDerm EFT-306 skin tissue reconstruct (A) and an EpiAirway AIR-606 lung tissue reconstruct (B).

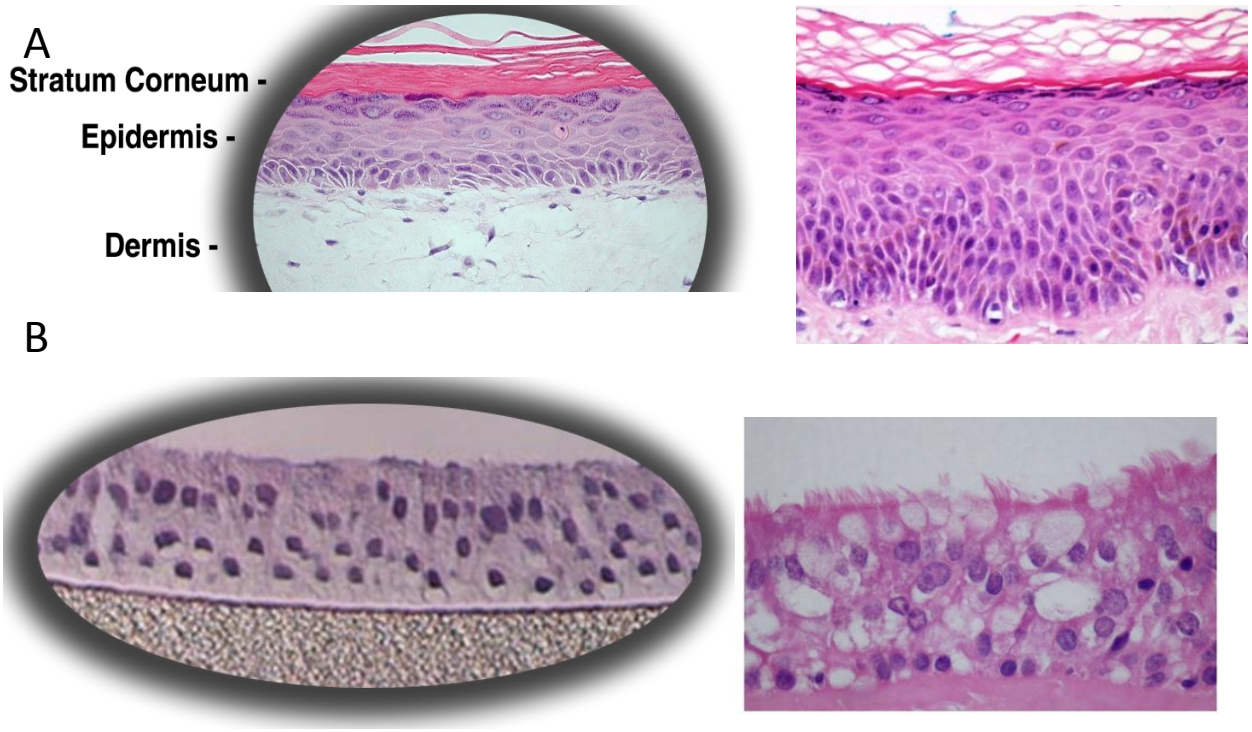


**Figure 3**. A side-by-side comparison of the cross-sectional histology of the normal EpiDerm EFT-306 skin reconstruct (left) and normal human epidermis (TissuPath, Mount Waverely, AU) (right)(A); as well as EpiAirway AIR-606 lung reconstruct (left) and human tracheal epithelium (Wright *et al.*, 2008) (right) (B).

*2.2.1 Skin Tissue Reconstructs*

The EFT-306 full thickness skin reconstructs consist of normal human fibroblasts (NHDF) embedded in a collagen layer (representing the skin dermis) plated on top of the insert membrane.

Normal human keratinocytes (NHEK) are grown on top of the dermal layer to form 8-12 cell layers (basal, spinous, and granular layers) along with a stratum corneum. These cells are derived from a single donor of neonatal-foreskin tissue. The reconstructs were grown in Millicell single-well tissue-culture inserts (PTFE membrane pore size 0.4 µm, inner diameter 2.2 cm, surface area 4.2 $cm^2$; Millipore PICMORG 50) with 1 mL of media underneath the insert membrane.

*2.2.2 Lung Tissue Reconstructs*

The AIR-606 lung reconstructs are comprised of normal human tracheal/bronchial epithelial cells (NHBE). These are derived from the respiratory tract of a single donor, non-smoker, and free of respiratory tract disease. Each reconstruct consists of 3-4 cell layers in a pseudo-stratified morphology, has a ciliated human bronchiole-like structure, and mucin producing goblet cells as well as Clara cells. The lung reconstructs were grown in Millicell single-well tissue-culture plate inserts (PTFE membrane pore size 0.4 µm, inner diameter 2.2 cm, surface area 4.2 $cm^2$; Millipore PICMORG 50) with 1 mL of media (AIR-100-ASY-PRF, MatTek) under the insert membrane.

**2.3 Benzene Exposure Protocol and Sample Collection**

Both skin and lung reconstructs were exposed to benzene concentrations of 30 ppm, 60 ppm, and 120 ppm for 6 h per day for 5 consecutive days. Clean-air exposure reconstructs were used to identify potential effects of air-flow and contaminants in the *in vitro* exposure system. An unexposed age control was included for both the lung and skin reconstructs to account for potential changes in the tissue integrity due to developmental changes of the reconstructs during the staggering of the timing of the exposure experiments. The unexposed age control was left in the incubator for the duration of the experiment. Between the daily exposures, the treated reconstructs were returned to the incubator.

The benzene exposure concentrations were selected based on the concentrations that were observed during human exposure scenarios (ATSDR, 2007; Midzenski *et al.*, 1992; Yin *et al.*, 1987). Our exposure system delivered a stable benzene vapor concentration to the exposure chamber for the duration of the experiments (Figure 4). The exposure chamber settings utilized for the different benzene exposure concentrations are summarized in Table 1.

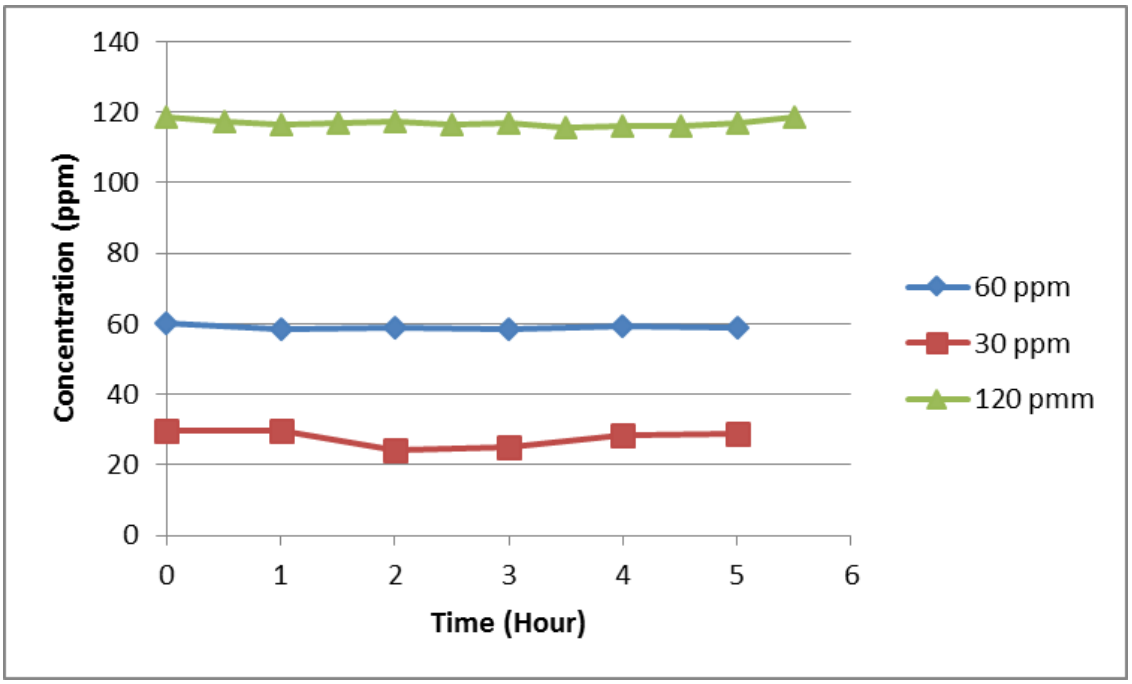


**Figure 4**. A sample representation of exposure chamber benzene vapor concentrations as measured by the Varian CP-3800 GC.

**Table 1**. The exposure-chamber system settings during the clean air and benzene exposure regimens.

| | Lung Reconstructs | | Skin Reconstructs | |
|---|---|---|---|---|
| | Clean air & 120 ppm benzene | 30 & 60 ppm benzene | Clean air & 120 ppm benzene | 30 & 60 ppm benzene |
| Rotameter Temperature (C$^o$) | 53 | 42 | 53 | 42 |
| Rotameter Chamber Flow (L/min) | 0.4 | 0.375 | 0.4 | 0.4 |
| Dilution Air Flow Control (L/min) | 3.75 | 3.75 | 3.75 | 3.75 |
| Flow Controller 1 (L/min) | 1.04 | 0.92 | 1.04 | 1.32 |
| Flow Controller 2 (L/min) | 0.70 | 0.52 | 0.53 | 0.53 |
| Flow Controller 3 (L/min) | 1.40 | 1.00 | 1.32 | 1.32 |
| Vacuum Flow Controller (L/min) | 3.00 | 2.75 | 2.50 | 2.51 |
| $CO_2$ Tank Flow Controller (L/min) | 1.00 | 1.00 | 1.00 | 1.00 |
| High Concentration Chamber Flow (L/min) | 1.00 | 1.00 | 1.00 | 1.00 |
| Low Concentration Chamber Flow (L/min) | 1.50 | 1.00 | 1.00 | 1.00 |
| Dew point (C$^o$) | 18.9 | 19.0 | 20.1 | 20.6 |

Skin and lung reconstructs were exposed to clean air or benzene for 6 hours per day for 5 consecutive days by placing the 6-well plate containing two or three reconstructs within the center of the exposure chamber to ensure an even exposure distribution across the reconstructs. Separate exposure experiments were carried out for the lung and skin reconstructs. Reconstructs were placed in the A and B positions as shown in Figure 5. The C well was only used in the 120-ppm exposure experiment when an unwashed lung reconstruct was included in the experiment (Figure 5). The exposure experiments were conducted over a 2-week period. Because of the limited number of exposure chambers (2), tissues could be exposed to only two doses per week. Reconstructs were exposed to clean air or 120 ppm benzene vapor during week 1 while, during week 2, another set of reconstructs were exposed to 30 ppm or 60 ppm of benzene vapor. The unexposed control was grouped with the week 2 exposures in order to observe how aging effects of aging on the reconstructs

Media was collected from each well prior to treatment each day for LDH analysis (see below) and the volume was recorded. This was necessary due to loss of media from evaporation during treatment. LDH results were normalized to volume of media. Pre-exposure media samples were collected for each reconstruct for base-line LDH levels and daily post-exposure samples were collected 24 h after each exposure to measure cell membrane damage due to daily exposures. New media (1 mL) was added to each well before exposure. The collected media was stored in the -20$^{o}$C freezer until analysis. Before each exposure, the lung reconstructs were washed with phosphate buffed saline (PBS) solution 4-5 times to remove the mucous that is continuously generated by the reconstructs. To investigate if washing of the reconstruct prior to exposure potentially affected the toxicity profile, one unwashed lung reconstruct was included in the highest benzene exposure experiment (120 ppm) (position C in the 6-well plate; Figure 5).

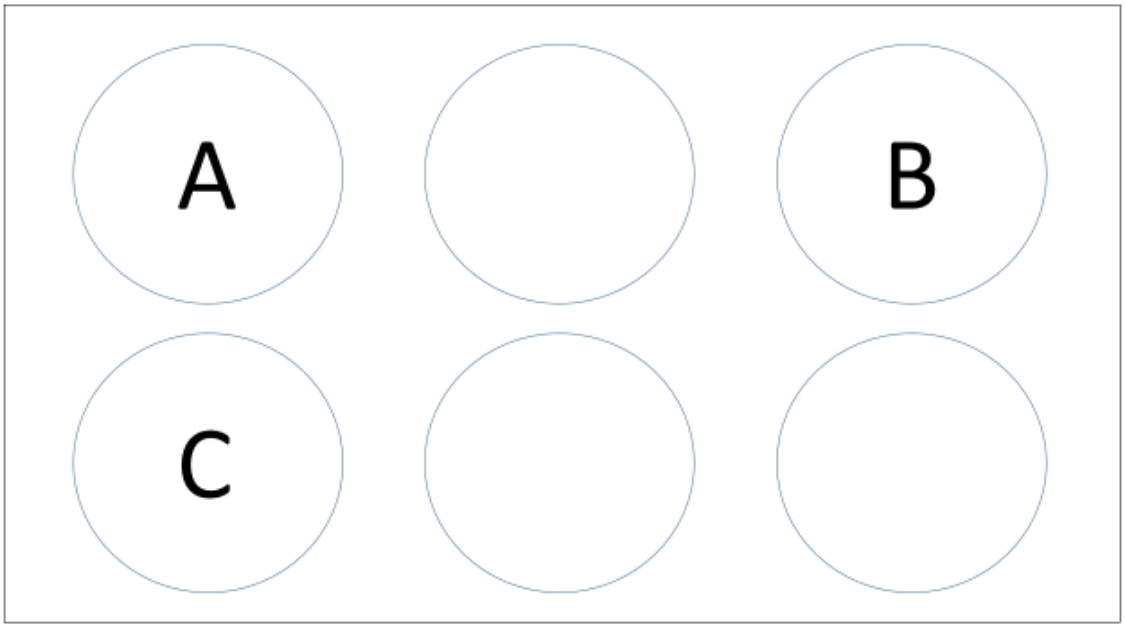


**Figure 5**. A diagram depicting the positioning of the reconstruct inserts within the 6-well plate in the benzene vapor exposure chamber. Wells A and B were used for both skin and lung reconstructs at all exposure concentration while well C was only used for the washed lung reconstruct at 120 ppm benzene exposure.

## 2.4 Analysis of the Skin and Lung Constructs

At the end of the 5-day exposure, the reconstructs were prepared for analysis. For each dose, the A position reconstruct was fixed for histological staining as were the unexposed age control and unwashed lung reconstruct.

### *2.5.1 Histological Staining*

We used hematoxylin and eosin staining (H&E staining) to investigate the potential morphological changes due to exposure to clean air and benzene. A Leica ST5010 Autostainer XL was used by the UNC Translational Pathology Laboratory to stain the buffered formalin-fixed and paraffin-embedded reconstructs using the H&E regressive protocol (see Table 2). After staining, we analyzed the slides of the reconstructs to determine the effect of benzene exposure on the morphology of the reconstructs.

In addition to the H&E staining, we stained the lung reconstructs with a Periodic acid–Schiff (PAS) stain with a hematoxylin counterstain. The PAS stain highlights structures containing mucins and glycogen that would allow us to detect the goblet cells in the lung reconstructs. We performed the PAS staining following the protocol in Table 3 and mounted coverslips using Cytoseal 60.

**Table 2**. The H&E regressive staining protocol used for the skin and lung reconstructs.

| Step Number | Station Number | Reagent | Time |
|---|---|---|---|
| 1 | Oven | N/A | 15 min |
| 2 | 1 | Xylene | 10 min |
| 3 | 2 | Xylene | 5 min |
| 4 | 3 | Xylene | 3 min |
| 5 | 4 | 100% ETOH | 1 min |
| 6 | 5 | 100% ETOH | 1 min |
| 7 | 6 | 95% ETOH | 1 min |
| 8 | Wash 1 | $H_2O$ | 2 min |
| 9 | 8 | Hematoxylin | 4 min |
| 10 | Wash 5 | $H_2O$ | 1 min |
| 11 | 9 | Clarifier 2 | 1 min 30 sec |
| 12 | Wash 4 | $H_2O$ | 1 min |
| 13 | 10 | Bluing | 40 sec |
| 14 | Wash 3 | $H_2O$ | 1 min |
| 15 | 11 | 95% ETOH | 1 min |
| 16 | 12 | Eosin-Y | 40 sec |
| 17 | 13 | 100% ETOH | 1 min |
| 18 | 14 | 100% ETOH | 1 min |
| 19 | 15 | 100% ETOH | 1 min |
| 20 | 16 | Xylene | 1 min |
| 21 | 17 | Xylene | 1 min |
| 22 | 18 | Xylene | 1 min |
| 23 | Exit | Xylene | 1 min |

**Table 3**. The PAS staining protocol used for the lung reconstructs.

| Step Number | Station Number | Reagent | Time |
|---|---|---|---|
| 1 | 1 | Xylene | 10 min |
| 2 | 2 | Xylene | 10 min |
| 3 | 3 | 100% ETOH | 3 min |
| 4 | 4 | 100% ETOH | 3 min |
| 5 | 5 | 95% ETOH | 3 min |
| 6 | 6 | 95% ETOH | 3 min |
| 7 | 7 | 70% ETOH | 3 min |
| 8 | 8 | 70% ETOH | 3 min |
| 9 | Rinse | Tap Water | 3 min |
| 10 | Rinse | DI $H_2O$ | 3 min |
| 11 | 9 | Periodic Acid Solution | 5 min |
| 12 | Wash 1 | Distilled $H_2O$ | 3 min |
| 13 | 10 | Schiff's Reagent | 15 min |
| 14 | Wash 2 | Tap Water | 5 min |
| 15 | 11 | Hematoxylin Solution | 45 sec |
| 16 | Wash 3 | Tap Water | 3 min |
| 17 | Rinse | DI $H_2O$ | 3 min |
| 18 | Rinse | Tap Water | 3 min |
| 19 | 8 | 70% ETOH | 3 min |
| 20 | 7 | 70% ETOH | 3 min |
| 21 | 6 | 95% ETOH | 3 min |
| 22 | 5 | 95% ETOH | 3 min |
| 23 | 4 | 100% ETOH | 3 min |
| 24 | 3 | 100% ETOH | 3 min |
| 25 | 2 | Xylene | 10 min |
| 26 | 1 | Xylene | 10 min |

*2.5.2 LDH Assay*

We used the LDH assay to quantify the amount of cell death exhibited by the reconstructs during the exposures. LDH is a soluble cytosolic enzyme that is release into culture medium as a result of the loss of cell membrane integrity from either apoptosis or necrosis. The assay measures LDH in the medium via a two-step reaction. First, the LDH catalyzes the reduction of $NAD^+$ to NADH and $H^+$ through the oxidation of lactate to pyruvate. During the second step diaphorase uses the NADH and $H^+$ to catalyze the reduction of a tetrazolium salt to a highly-colored formazan which absorbs energy readily at 490-520nm (Cayman Chemical Company, Ann Arbor, MI). We used an

amended version of the Cayman LDH protocol (Cayman Chemical Company, Ann Arbor, MI). To conserve kit materials, half of the recommended volume of samples and reagents were used (*i.e.*, 50 µL *vs.* 100 µL). Preparation of the standards was adjusted by using the tissue culture media to reconstitute the LDH standards instead of the described buffer solution. The tissue culture media was used to account for background color (phenol red) that the media contributed to the assay measurements. Furthermore, four additional LDH standard concentrations were added to the skin reconstructs standard curve and three concentrations were added to the lung reconstruct standard curve to supplement the specified dilutions to create a linear standard curve. The concentrations specified in the manufacturer's protocol were too high to produce a linear curve. The LDH concentrations used to produce the standard curve are detailed in Table 4.

**Table 4**. The LDH concentrations used for the standard curves for both lung and skin reconstructs. (*dilutions added to the protocol)

| **LDH Standards (mU/mL)** | |
|---|---|
| Lung Reconstructs | Skin Reconstructs |
| 10 | 10 |
| 5 | 5 |
| 2.5 | 2.5 |
| 1.25 | 1.25 |
| 0.625 | 0.9375* |
| 0.3125* | 0.625 |
| 0.16125* | 0.46875* |
| 0.078125* | 0.3125* |
| 0 | 0.16125* |
| - | 0.078125* |
| - | 0 |

The LDH standard concentrations were adjusted to account for the effect of phenol red in the culture media on the background readings. The lung reconstruct medium lacked phenol red, but the skin medium contained the indicator dye. The standard curves created from these standards are presented in Figures 6 and 7. While theoretically the intercept should be zero for the standard

curves, readings at low absorbances are not accurate (Caprette, 2012). This has been observed in multiple LDH standard curves that accompany LDH assay kits, such as the Cayman LDH Cytotoxicity Assay Kit (Cayman Chemical Company, 2012). After 30-min reaction time at room temperature, absorbance of each plate was read at 490 nm wavelength using a Molecular Devices Emax precision microplate reader.

In order to establish maximum threshold for the LDH analysis, we treated cells to ensure 100% kills. Two different methods, freeze/thaw and detergent, were used to lyse cells in both the skin and lung reconstructs. For the freeze/thaw method the reconstruct was place in a 15 mL centrifuge tube with 1 mL of the appropriate media and then placed into a freezer (-80$^{o}$C) for 30 min. and then thawed at room temperature for 30 minutes. This procedure was repeated. The tube of lysed cells was vortexed and centrifuged at 3000 x g before the media was removed and stored at -20$^{o}$C. For the detergent method we incubated the reconstructs in 2mL of 5% Triton X-100 for 18 h. After 18 hours the detergent and media were removed and the media being stored at -20$^{o}$C in a glass vial. For LDH analysis, these samples were diluted fourfold to lower the absorbance to levels measurable on the standard curve.

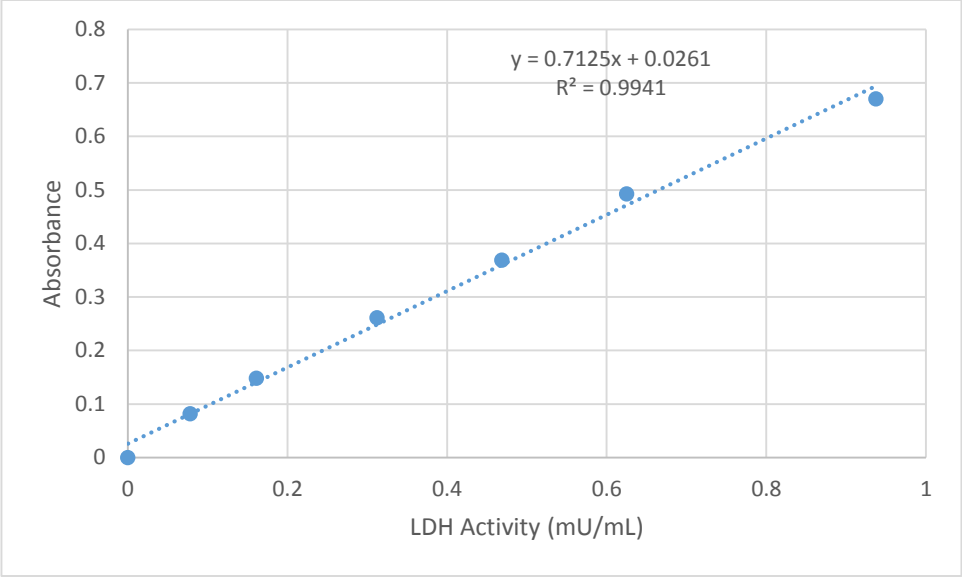


**Figure 6**. The LDH assay standard curve using the skin reconstruct culture medium.

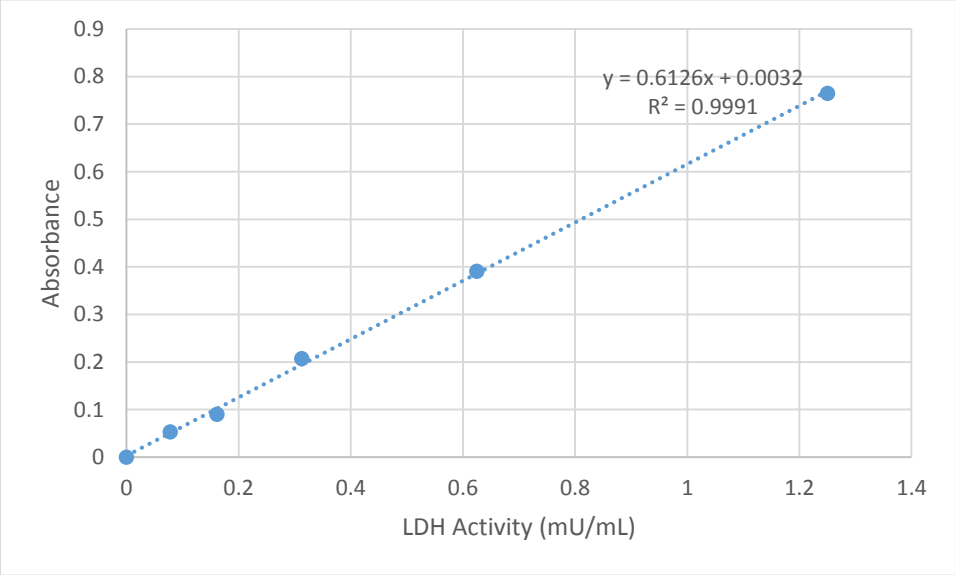


**Figure 7**. The LDH assay standard curve using the lung reconstruct culture medium.

### 2.6 Statistical Analyses

Each media sample was measured in duplicate for accuracy. Before averaging the duplicate measurements each sample was normalized to the sample volume these normalized values were then averaged. Once the absorbance for each sample was determined we calculated the LDH activity for each sample using the equations obtained from the standard curves (Figures 6 and 7).

Using the Student's t-test we compared the effects of air exposure, age of reconstruct, position in the chamber, and benzene exposure for the reconstructs. The Student's t-test revealed no significant difference ($p < 0.05$) between the LDH activities of the A and B reconstructs. Therefore, we averaged the LDH activities of the A and B reconstructs for each exposure and treated them as one exposed tissue for the analysis. The LDH activities of the exposed reconstructs were plotted for each day of the exposure (Figures 11 and 13).

## 3. Results

### 3.1 Tissue Morphology

The H&E stained cross-sections of the benzene and the clean-air exposed skin reconstructs are presented in Figure 8. The H&E stained skin reconstructs show the stratum corneum (the outer layer of dark pink keratin), the epidermal layer (light pink below the stratum corneum), and the dermal layer (white/clear below the epidermal layers). Going from outer to inner epidermal layers, the skin reconstruct consists of the stratum corneum, the stratum granulosum, stratum spinosum, and stratum basale cells found in human skin tissue. The skin reconstructs exposed to clean air, 30 ppm, 60 ppm, and the unexposed-age control were all similar in thickness (Figure 8A – D). The slight increase in thickness of the stratum corneum in the reconstructs exposed to 120 ppm of benzene may indicate a protective response (Figure 8D). However, since this interpretation is based on only one experiment, this observation would need to be confirmed with more samples.

The H&E stained cross-sections of the lung reconstructs are presented in Figure 9. The cross sections of the lung reconstructs show only one cell type, bronchial epithelial (light pink), after H&E staining. MatTek states that their lung reconstructs have bronchial epithelium ciliated and unciliated, Clara, and goblet cells. However, it is difficult to distinguish between the multiple cell types with the H&E stain. The reconstructs exposed during Week 2 of the study (Figures 9A, C, and D) show development of ciliated cells that are absent in the reconstructs exposed during Week 1 (Figures 9B, E, and F). The ciliation of the reconstruct indicates increased maturation and differentiation of the lung reconstruct. The benzene exposed lung reconstructs (Figures 9C – F) exhibit a hypoplastic effect when compared to both the incubator and air control (Figures 9A – B).

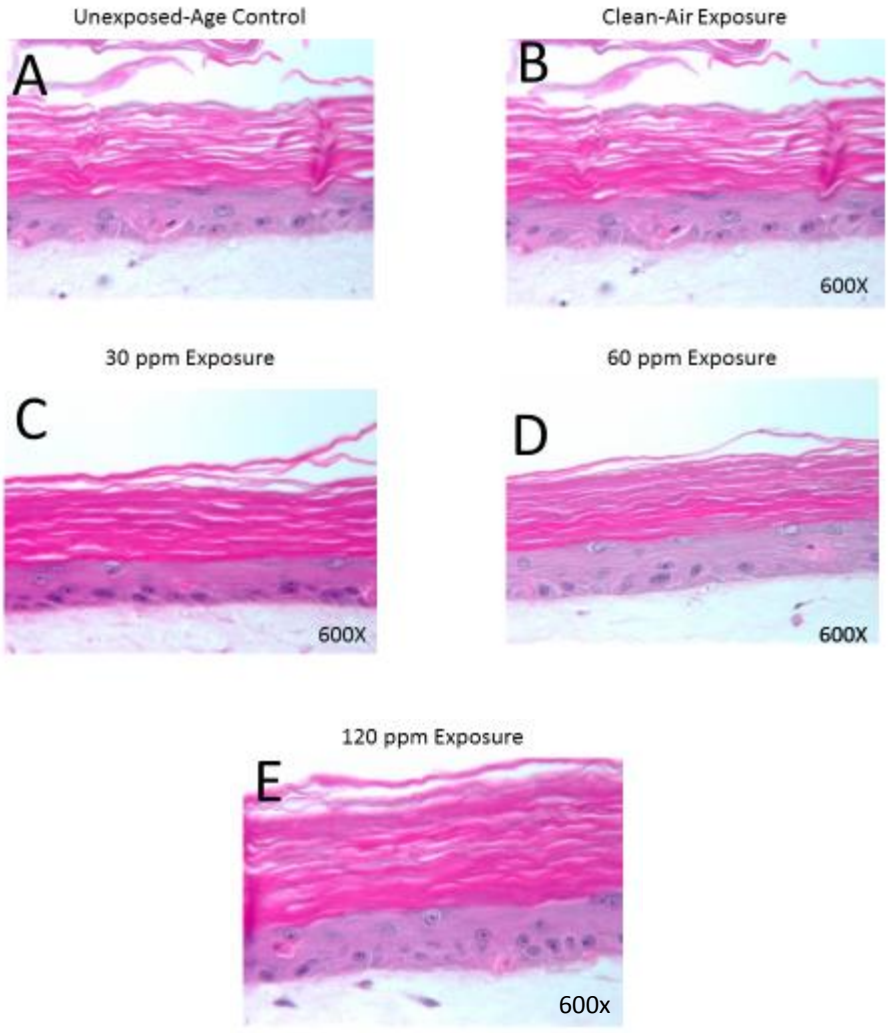


**Figure 8**. Cross sectional H&E staining of the unexposed-age control skin reconstruct (A) and the skin reconstructs after exposure to clean air (B) or benzene vapor at 30 ppm (C), 60 ppm (D), or 120 ppm (E).

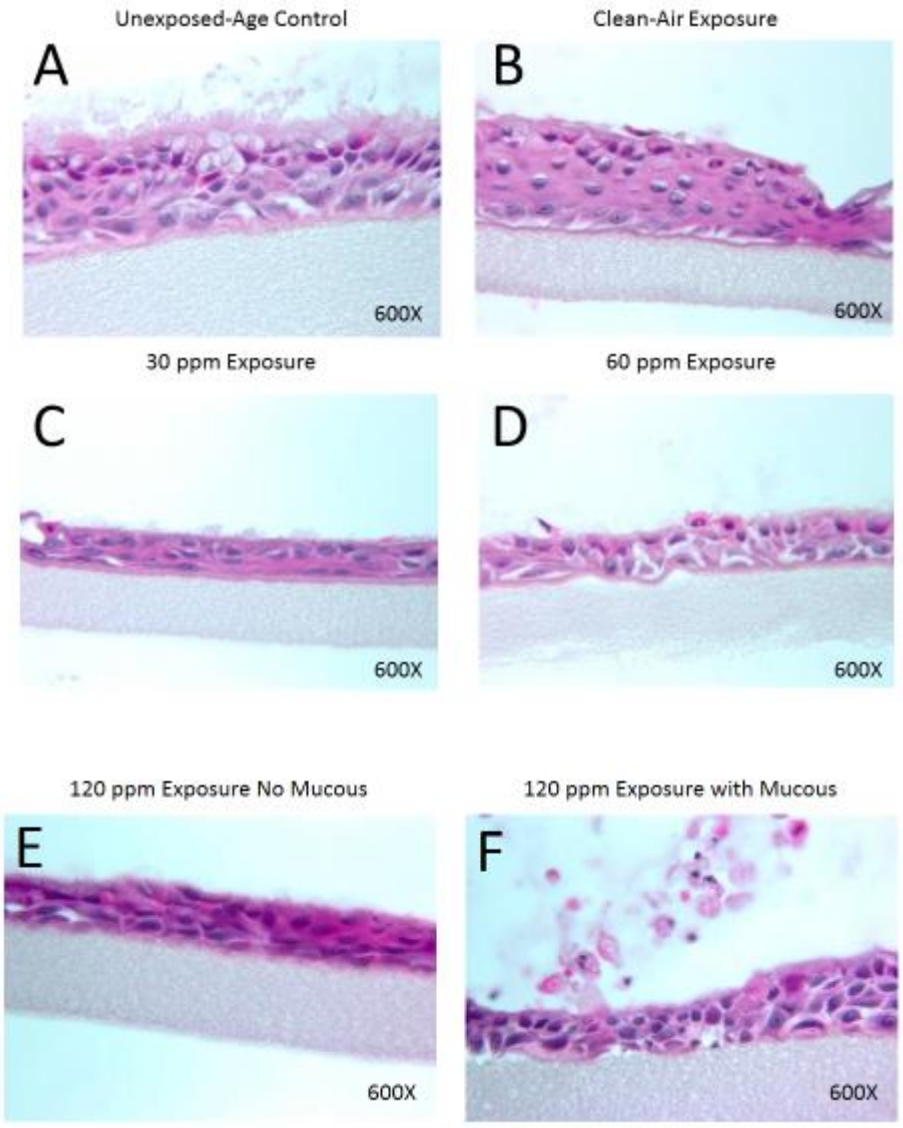


**Figure 9**. Cross sectional H&E staining of the lung reconstructs without any exposure (A; *i.e.*, incubator control) or after exposure to clean air (B), benzene vapor, 30 ppm (C), 60 ppm (D), or 120 ppm without mucous (E) or with mucous (F).

Lung reconstructs were also stained with PAS to determine the effect of benzene exposure on goblet cells (Figure 10). The goblet cells are stained pink in the cross sections of the lung reconstructs with the rest of the tissue stained purple (hematoxlyin). Arrows indicate positions of the goblet cells (Figures 10A – C). The reconstructs that were exposed to benzene lack goblet cells (Figures 10D – F) compared to the clean-air exposed, unexposed-age, and human bronchial epithelium (Figures 10A – C & G). The lack of goblets cells correlates positively with an exposure to benzene in reconstructs without mucous. The unwashed 120 ppm mucous reconstruct was the only benzene exposed tissue with goblet cells indicating the mucous serves as a protective barrier for the lung reconstructs.

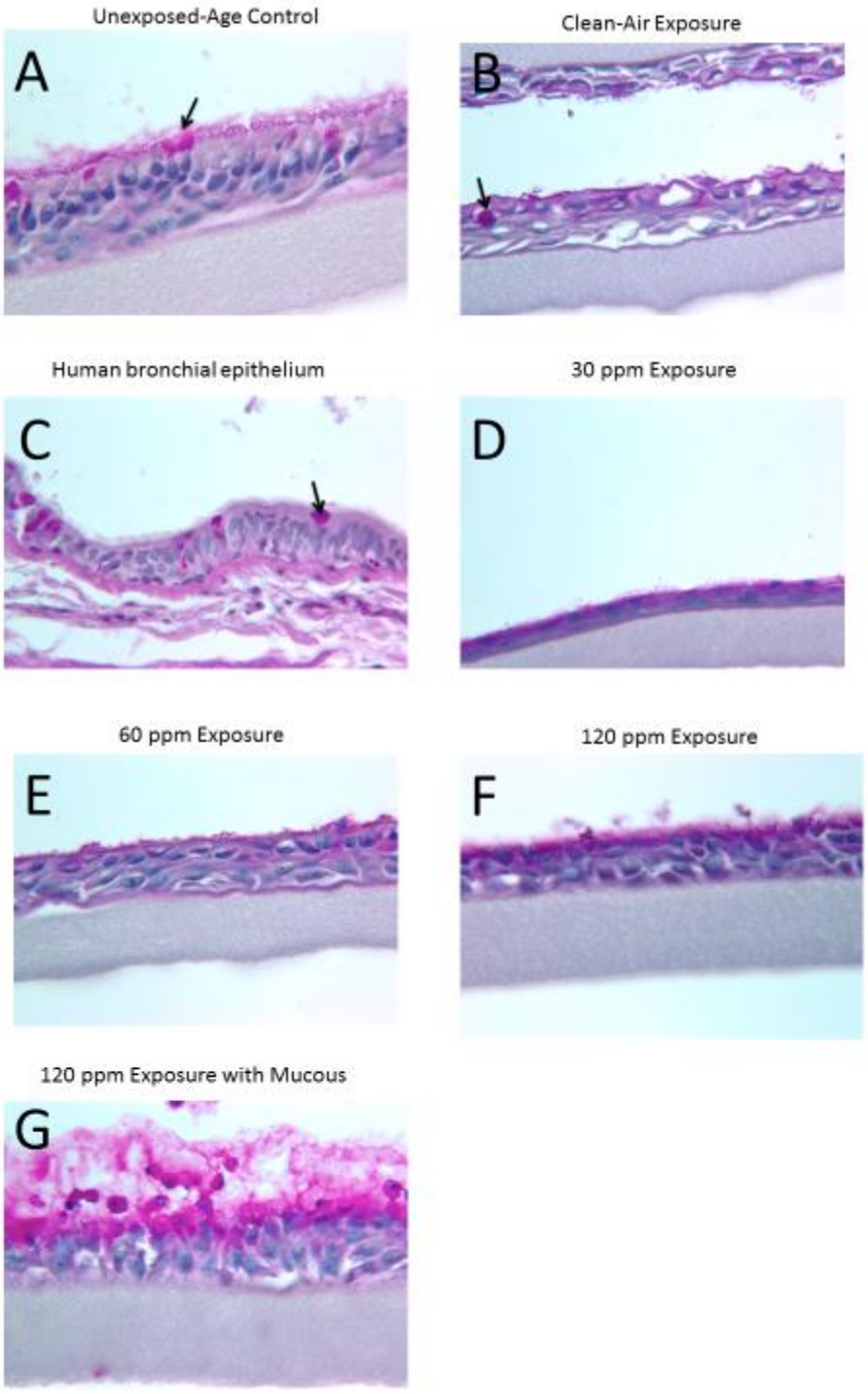


**Figure 10**. Cross sectional PAS staining of the lung reconstructs (600X) without any exposure (A; *i.e.*, incubator control) or after exposure to clean air (B), normal human bronchial epithelium (C), benzene vapor, 30 ppm (D), 60 ppm (E), or 120 ppm without mucous (F) or with mucous (G).

### 3.2 LDH Activity

The LDH activity of the skin reconstruct medium was measured before the first exposure (Day 1) and 24 hours after each exposure (days 2 – 6) (Figure 11). For duplicate exposures (i.e. A and B slots) the volume normalized LDH activity for the two samples was averaged. The LDH activity pattern for the 5 skin reconstruct exposure groups show an initial increase of the LDH activity at the beginning of the exposure following a gradual decrease in activity resulting in a plateauing of LDH activity by the end of the week (Figure 11). A significant difference in the LDH activities was observed between the unexposed-age (older) and the clean air control (younger) skin reconstructs after the first day of exposure (Figure 12). This evidence suggests that the age of the tissue does not affect LDH activity in the skin reconstructs while the clean air exposure increases LDH activity. No significant difference in LDH activity between the unexposed and clean air reconstructs was observed on Day 4 of the exposure perhaps due to the greater variability in the clean-air exposed samples (Figure 12). Because the exposure conditions were consistent, we suspect that the reconstructs have some inherent variability.

The overall LDH activity pattern for the 6 lung reconstruct exposure groups show an initial increase of the LDH activity at the beginning of the exposure week followed by a gradual decrease in activity each day resulting in a plateauing of LDH activity by the end of the week. However, the LDH activity range in the reconstructs exposed during the first exposure week (clean-air exposed and 120 ppm exposed) was up to an order of magnitude higher than that of reconstructs exposed the second week (30ppm, 60ppm and age controls) (Figure 13), with a significant difference observed between the unexposed and the clean air exposed reconstructs (Figure 14). There was no significant difference between the unexposed and clean-air exposed reconstructs on days with greater variability in the LDH activity of the clean-air reconstructs (Figure 14). As a

result, for the lung reconstructs we used the incubator control for comparison of the 30 ppm and 60 ppm exposed reconstructs and the clean air controls for comparison with the 120 ppm reconstructs. There was significant difference observed between both the 30 ppm and 60 ppm exposed reconstructs to the unexposed-age control (Figure 13). Furthermore, the LDH activity of both the A and B reconstructs for each exposure concentration were plotted for each day (Figures 15-19). These figures indicate that for every exposure, excluding the clean air exposure, the reconstruct in the A position had a slightly higher LDH activity than the B reconstruct with the 30 ppm samples varying more.

The positive controls (100% kill) for both the skin and lung reconstructs had LDH activities fourfold higher than those seen in the exposed tissues. This difference between these LDH activities indicates that our exposures resulted in cell death that was much lower than the potential maximum.

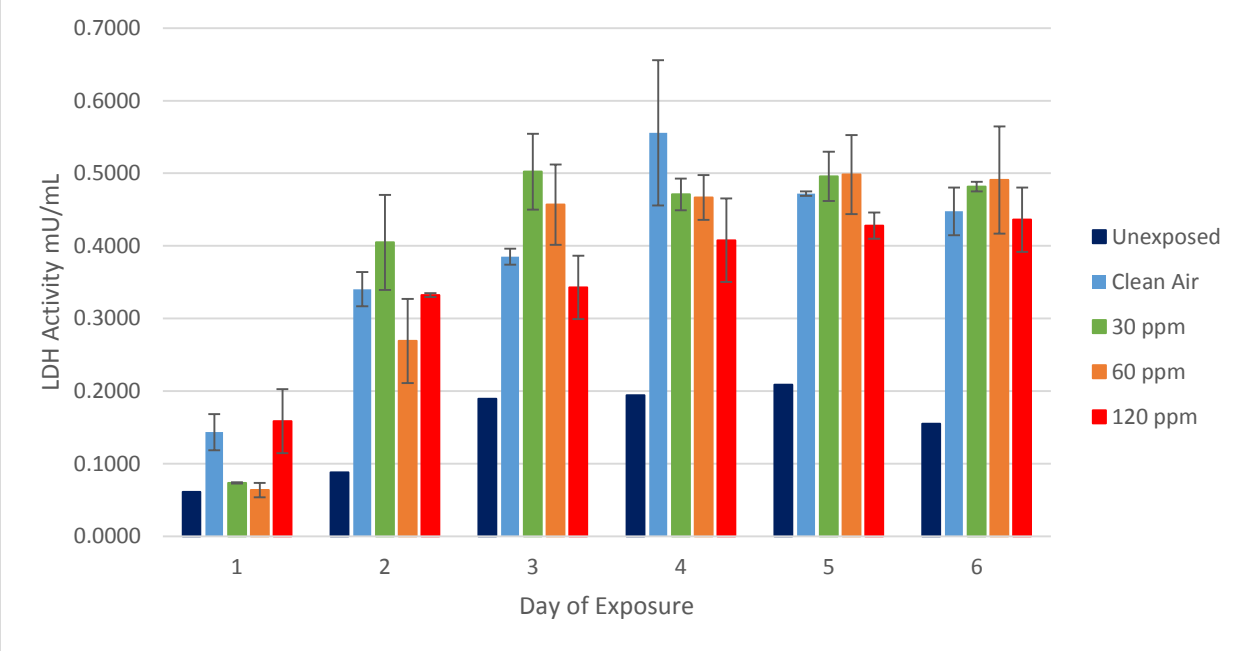


**Figure 11**. LDH activity in the culture medium of the skin reconstructs before the first exposure (Day 1) and 24 hours after each exposure (days 2 – 6).

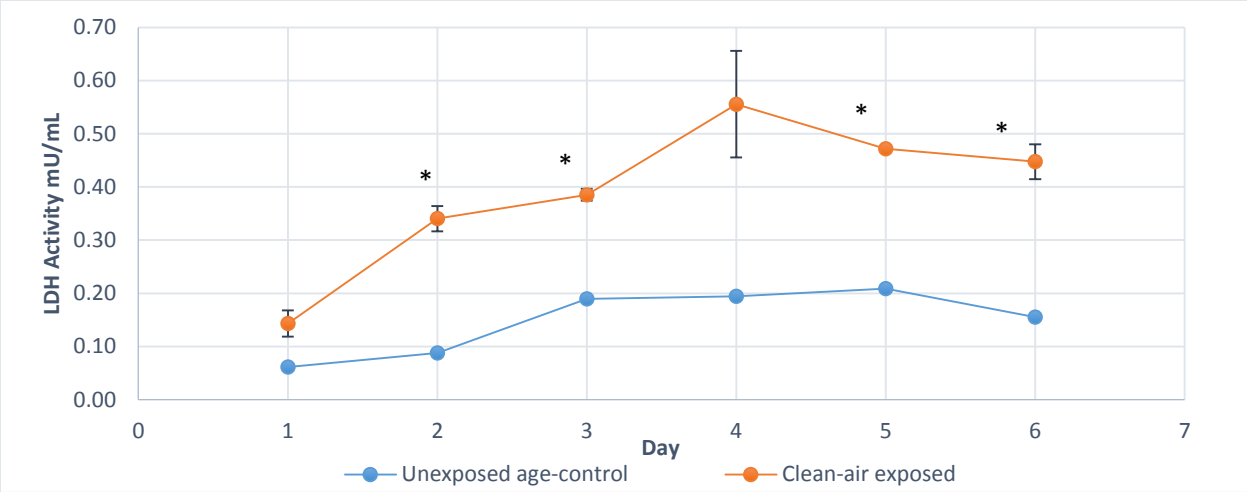


**Figure 12**. LDH activity in the culture medium of the unexposed age control and the clean air-exposed skin reconstructs before the first exposure (Day 1) and 24 hours after each exposure (days 2 – 6). * $p < 0.05$ when compared to the unexposed age control.

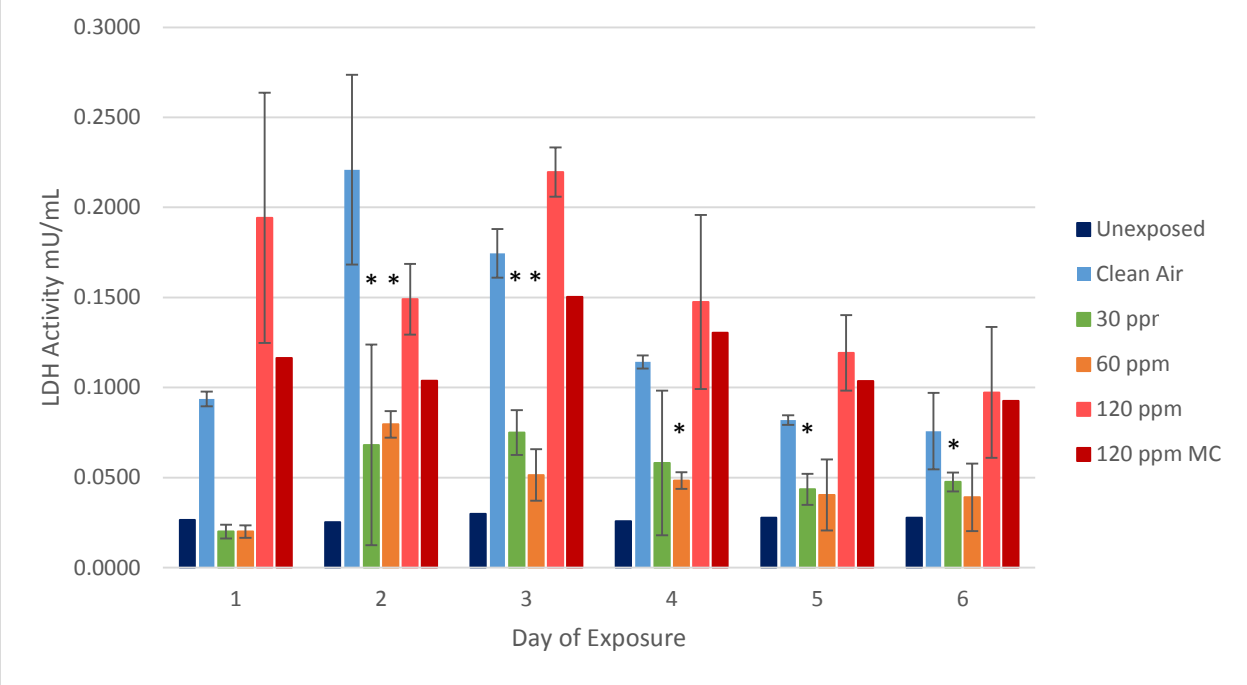


**Figure 13**. The measured LDH activity in the lung reconstruct culture medium before the first exposure (Day 1) and 24 hours after each exposure (days 2 – 6). * $p < 0.05$ when compared to the unexposed-age control.

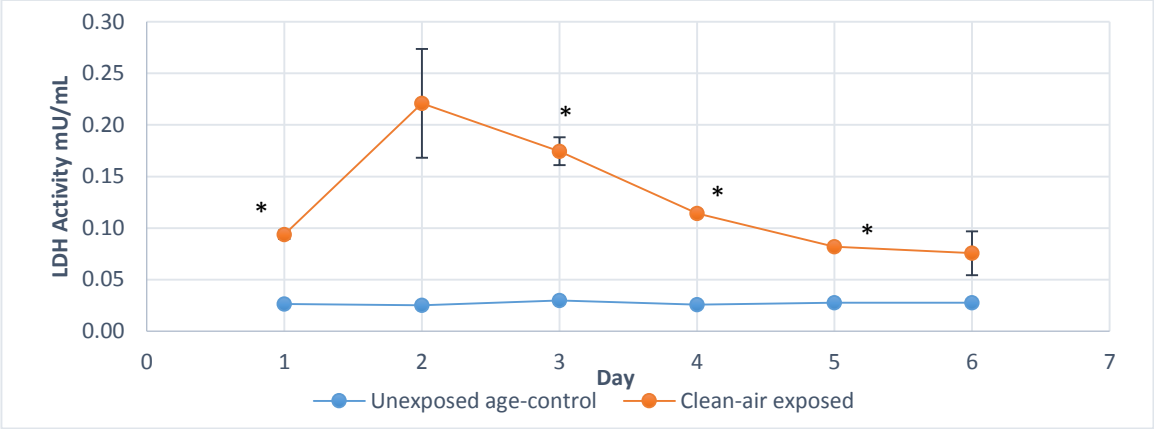


**Figure 14**. The measured LDH activity in the unexposed-age control (n = 1) and clean-air exposed (n = 2) lung reconstructs before each day of exposure (Day 1-5) and 24 h after the last exposure (Day 6). * $p < 0.05$

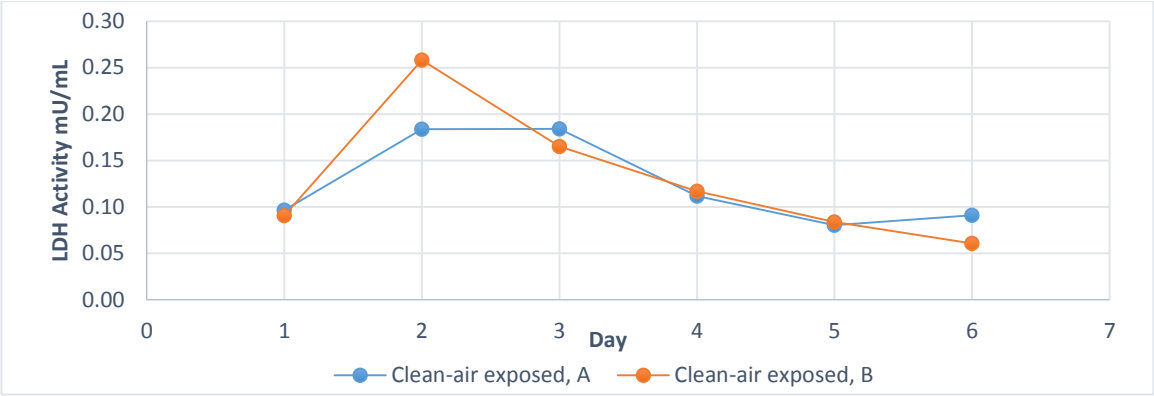


**Figure 15**. The measured LDH activity in the clean-air exposed A and clean-air exposed B lung reconstructs before each day of exposure (Day 1-5) and 24 h after the last exposure (Day 6).

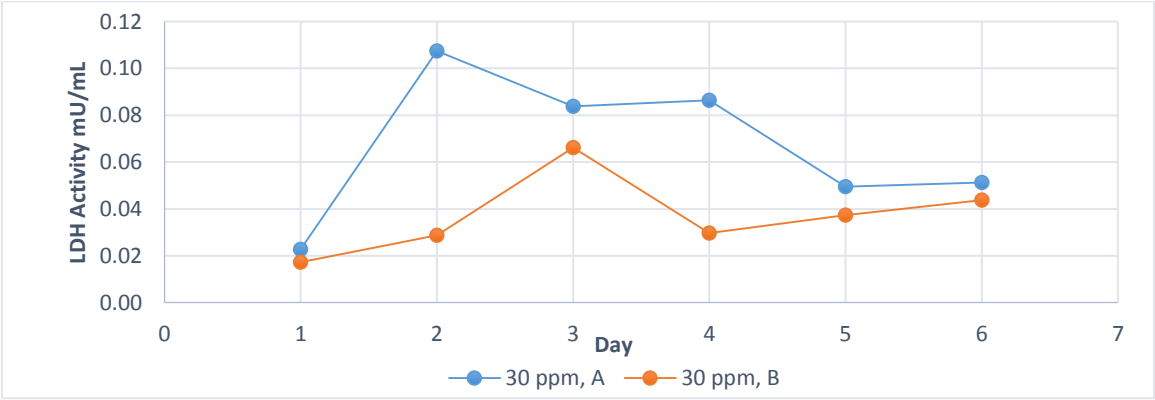


**Figure 16**. The measured LDH activity in the 30-ppm exposed A and B lung reconstructs before each day of exposure (Day 1-5) and 24 h after the last exposure (Day 6).

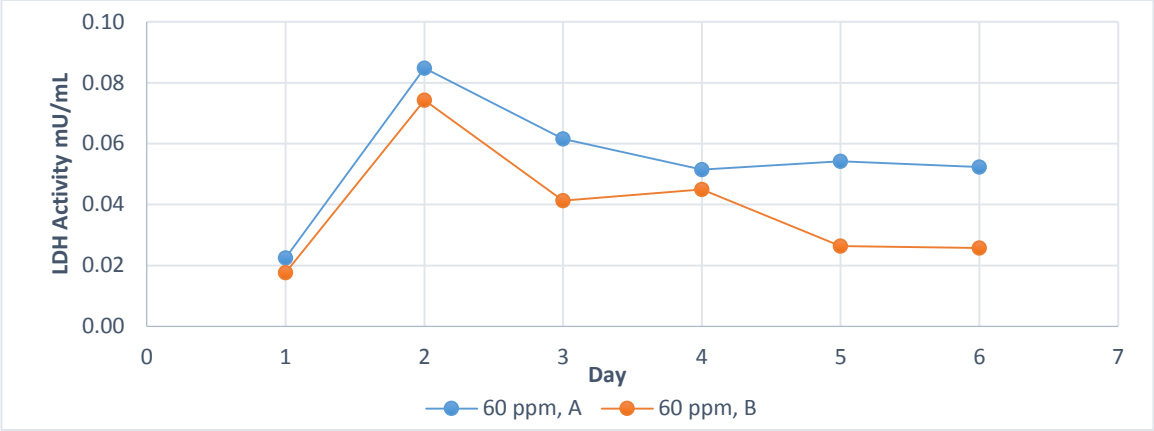


**Figure 17**. The measured LDH activity in the 60-ppm exposed A and B lung reconstructs before each day of exposure (Day 1-5) and 24 h after the last exposure (Day 6).

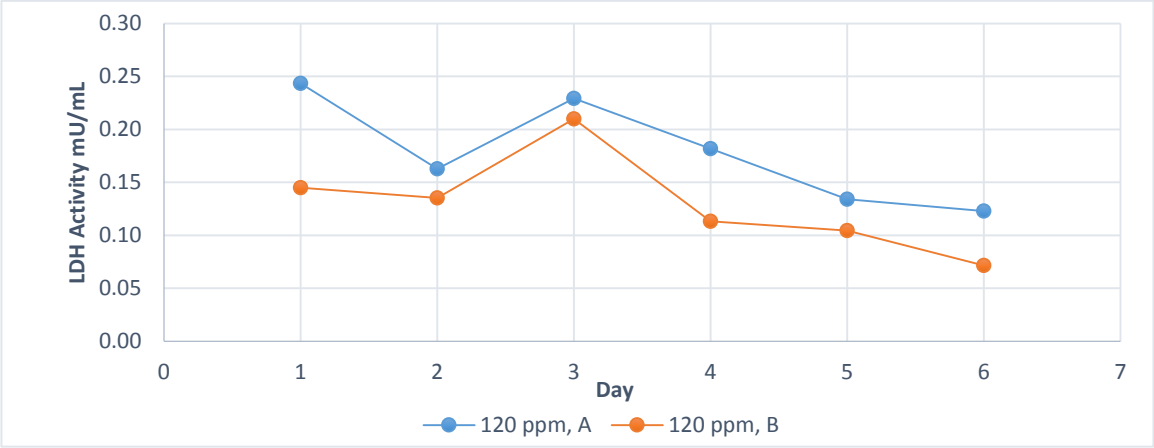


**Figure 18**. The measured LDH activity in the 120-ppm exposed A and B lung reconstructs before each day of exposure (Day 1-5) and 24 h after the last exposure (Day 6).

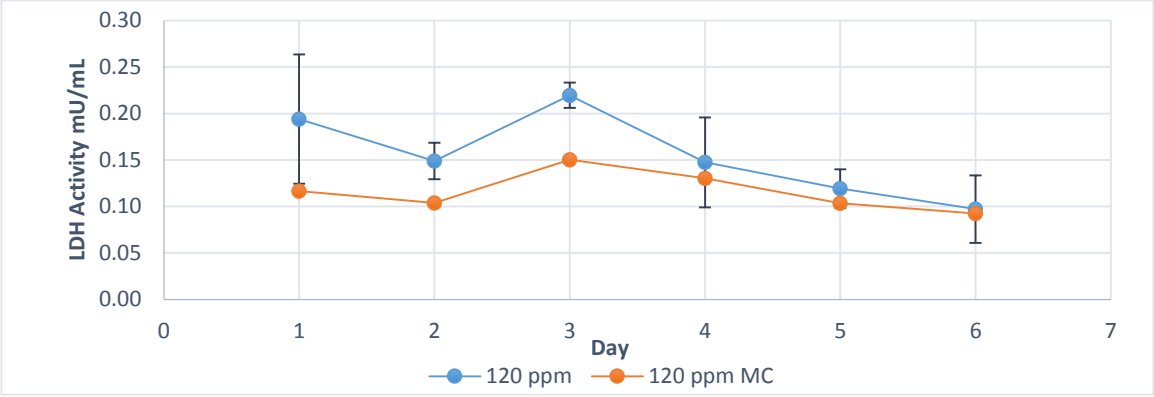


**Figure 19**. The measured LDH activity in the 120-ppm exposed lung reconstructs with and without mucous washing (MC) before each day of exposure (Day 1-5) and 24 h after the last exposure (Day 6).

## 4. Discussion

### 4.1 The Effect of Clean Air Exposure in the Reconstructs

The primary goal of my study was to validate the exposure-generation chamber system for *in vitro* exposure assessment and analysis of the effects of airborne benzene exposure in 3D human lung and skin reconstructs. To control for the effect of the exposure chamber condition on the measured cytotoxicity (i.e., LDH activity), we compared the LDH levels in the skin and lung reconstructs exposed to clean air to that of the unexposed age controls (Figures 12 and 14). The LDH activity in the unexposed age control, for both skin and lung reconstructs, was significantly less than in the clean-air exposed reconstructs (Figures 12 and 14). Both the skin and lung reconstructs also exhibited similar trends in LDH activity showing an initial rise in activity after the first day followed by a steady decline and plateauing by the end of the $5^{th}$ day of exposure. The increased LDH levels in the clean-air exposed reconstructs indicated that the conditions of the exposure chamber had an effect on the LDH activity in the reconstructs. While humidity was added to the air delivered to the exposure chambers, the added humidity was not sufficient for the reconstructs. Inside an incubator reconstructs are exposed to conditions at 95% relative humidity and according to the measured dew point we were able to deliver air with a relative humidity of ~80% to the exposure chambers. The lowered humidity could have dehydrated the reconstructs resulting in the increased LDH activity of the clean-air exposed reconstructs.

Additionally, the unexposed lung reconstruct (Figure 9A) developed ciliated cells over the course of the experiment but the air-exposed control did not. This limited cell differentiation in the clean-air exposed lung reconstructs correlated with the increased LDH activity observed in the clean-air exposed lung reconstructs. Also the unexposed lung reconstruct had more goblet cells than the clean-air exposed reconstruct (Figure 10 A&B). The observed difference in goblet cell

number between the unexposed and clean-air lung reconstructs could be a result of goblet cells differentiating into ciliated cells (Rogers, 1994). Ciliated cells are more sensitive to exposure conditions and apoptosis, so as ciliated cells died from the exposure goblet cells differentiated to replace them, thus resulting in a decreased number of goblet cells in the reconstructs. Furthermore, the clean-air exposed lung reconstructs located at the A and B positions had no significant difference in the LDH activity (Figure 15). The lack of variability in the LDH activities in the two clean-air lung reconstructs indicates that the conditions in the exposure chamber equally affected both reconstructs.

### 4.2 The Effect of Aging

Due to the availability of only two exposure chambers for our experiments, two weeks was required to complete the exposure for each reconstruct type. Clean-air and 120 ppm benzene exposures were carried out during the first week and the 30 ppm and 60 ppm exposures during the second week. To account for the difference in the age of the reconstructs, one unexposed skin and one unexposed lung reconstruct were maintained in the incubator for the duration of the 2-week experiment. Day 1, prior to exposure, LDH activity in the unexposed age and clean-air exposed reconstructs was used to determine the potential effect of aging. No significant difference was observed between the unexposed age and clean-air exposed skin reconstructs prior to the start exposure (Figure 12).

The range of LDH activity in the lung reconstructs exposed during week 1 (clean-air and 120 ppm exposed) was an order of magnitude higher than that of reconstructs exposed during week 2 (30 ppm, 60 ppm, and unexposed age control) (Figure 13). As exposure experiments were initiated a day after the arrival of the reconstructs, the increase in LDH activity on Day 1 (*i.e.*, prior to the start of the exposure) in the first week could be a result of the delivery conditions as

compared to those with a week of acclimation and stabilization in the incubator. Due to age, no perceivable differences were observed in morphology or indicators of damage between the unexposed age control and the clean-air exposed reconstruct (Figure 9A and B). However, there were less goblet cells present in the clean-air exposed reconstruct when compared to the unexposed age control (Figures 10A and B). The increase in goblet cells in the unexposed age control suggest that the additional week in the incubator allowed for increased cell differentiation in the lung reconstructs. With aging, degradation of cellular and reconstruct integrity is expected, thus resulting in an increase in LDH activity. The results indicate that one day between receiving the reconstructs and the start of the exposures may be insufficient for the reconstructs to return to homeostasis after stress induced by the shipping process and insufficient for the reconstructs to fully differentiate (Figure 9). The lack of maturation could explain the differences in the observed LDH activities between the lung reconstructs exposed during week 1 (clean-air and 120 ppm) and week 2 (unexposed, 30 ppm, and 60 ppm). Due to the differences between the LDH activity for week 1 and week 2, we used two reconstruct controls for comparison; 30 and 60 ppm exposed reconstructs were compared to the unexposed age reconstruct as a control while the 120 ppm exposed reconstructs were compared to the clean-air exposed reconstructs as a control.

### 4.3 The Effect of Benzene Exposure

I did not observe an effect of benzene exposure on the LDH activity in the skin reconstructs (Figure 11). There was no significant difference in the LDH activity between the clean-air and benzene exposed skin reconstructs. This agrees with the general understanding that the skin acts as an effective protective barrier towards many environmental exposures, including benzene vapor (Wester and Maibach, 2000). Even though the LDH activity in the skin reconstructs did not indicate a response to benzene exposure, the morphology of the 120 ppm exposed skin reconstruct

(Figure 8F) exhibited minor hyperkeratosis as evident by the increased thickness of the stratum spinosum layer in the reconstruct (Figure 8D) compared to the other skin reconstructs (Figure 8A-D). The hyperkeratosis observed in the 120 ppm exposed skin reconstruct could result from irritation from the benzene exposure.

In contrast to the skin reconstructs, I observed a cytotoxic effect of benzene exposure on the lung reconstructs (Figure 12). The 30 ppm and 60 ppm exposed lung reconstructs having LDH activities that were significantly higher ($p < 0.05$) from the unexposed-age control (Figure 12). An effect of benzene exposure was not observed in the 120-ppm exposed lung reconstructs when compared to the clean-air exposed reconstructs. The lack of difference between the 120 ppm exposed and the clean-air exposed reconstructs could be due to the stress induced from the shipping process (see above section 4.2). While the LDH activity in the 30 ppm and 60 ppm exposed lung reconstructs was different from the unexposed age control ($p < 0.05$), the LDH activities of the clean air, 30, 60 and 120 ppm exposed reconstructs were not statistically different from each other at $p < 0.05$. This indicates that these exposure concentrations were not sufficient to elicit a cytotoxic response in the lung reconstructs. The lung reconstructs exposed to 30 and 60 ppm of benzene had LDH activities that were significantly different from the 120 ppm exposed, but the lack of acclimation to the normal condition prior to the start of the exposure likely introduced bias to the results.

The LDH activity measured in the lung reconstructs that were placed in the A and B positions (Figure 5) in the 6-well plates indicated that the A position positively affected LDH activity, with reconstructs in the B position having a lower LDH activity for each day of the experiment (Figures 16, 17, and 18). When compared to their respective controls (clean-air exposed for 120 ppm, unexposed age control for 30 and 60 ppm) the lung reconstructs at the A

position had LDH activities significantly different from the controls while the B position tissues did not. However, this observed difference in LDH activity for reconstructs in the A and B position was not significantly different. This result indicates that the position of the reconstruct on the plate inside the exposure chamber may minimally affect the amount of exposure a reconstruct receives during an experiment. However, to confirm this finding further research is needed with reconstructs occupying each space in the 6-well plate. In addition, to placing reconstructs in each well of the 6-well plate measurements of the benzene concentration need to be taken from inside the exposure chamber. These measurements would confirm whether the benzene concentration was equal throughout the chamber.

Additionally, the lung reconstructs exposed to benzene showed minor hypoplasia (Figure 9). The four lung reconstructs exposed to benzene 30 ppm, 60 ppm, 120 ppm, and unwashed 120 ppm (Figure 9C - F) had a decreased number of cell layers compared to both the clean-air exposed and the unexposed age control (Figure 9A and B). The observed hypoplasia could be a result of cell death due to exposure to benzene. Cell death is clearly visible in the 120 ppm unwashed mucous lung reconstruct (Figure 8F) with the dead cells sloughing off with the mucous. The hypoplasia, in all benzene exposed lung reconstructs, correlates with the cell death incurred due to exposure to benzene. Furthermore, previous studies have indicated that increasing xenobiotic exposure dose results in decrease in cell numbers (Balharry et al. 2008). The loss of goblet cells is further indicative of cell death induced by benzene exposure (Figure 10). Goblet cells are only detected in the unexposed age control and clean-air exposed reconstructs (Figure 10A and B). However, to verify how benzene exposure affects lung reconstruct morphology, further studies should be performed to observe the morphological differences in the reconstructs before and after the exposure.

### 4.4 The Effect of Mucous in the Lung Reconstructs

The presence of the protective mucous layer had an observable, but not a statistically significant, effect on the LDH activity in the lung reconstructs (Figure 19). However, when the 120 ppm A position reconstruct was compared to the mucous control reconstruct, a significant difference in the LDH activity was observed. The difference of position in the 6-well plate could result in different exposures that may contribute to the variability observed in LDH activity. The statistically significant difference between the 120 ppm A and B reconstructs when compared to the 120 ppm mucous control supports the observation that the position of the reconstructs in the 6-well plate could affect the LDH activity of the reconstructs.

Furthermore, the lung reconstructs were observed to produce less mucous during the 24-h period between washings over the course of the experiment. Therefore, the reconstructs exposed during the first week of the experiment could have had an increased ability to produce mucous during the first days of the exposure, potentially explaining the reduction in the LDH activity during the second day of exposure (Figure 18 and 19). However, a decrease in the LDH activity was not observed in the clean-air exposed lung reconstructs, which were exposed during the same time. This different pattern in the LDH activity can, therefore, also indicate an inherent variability between the lung reconstruct samples. With the results obtained in this study, it is clear that the presence of mucous in the lung reconstructs has an effect on the measured LDH activity. However, it is unclear how mucous affects LDH activity because of other factors that could have influenced the observed LDH activity such as position, mucous production, and insufficient time to acclimate to incubator and/or chamber conditions. Further research with more stringent controls and methods needs to be carried out to understand how mucous affects LDH activity in the lung reconstructs.

### 4.5 Limitations of Experimental Design

During these experiments, we did not know if the week in the age difference between the two exposure groups could potentially affect the observed effects due to benzene exposure in the reconstructs, which necessitated our inclusion of an age control. The results suggests that the time difference does, indeed, affected the measured LDH concentrations in the medium because of the increased maturation and differentiation seen in the week 2 lung reconstructs. While we were restricted by the equipment available to us, in future experiments staggering of the ordering or growth of the reconstructs so that the reconstructs are the same age at the time of exposure is required. Additionally, all controls need to be exposed to the same conditions as the exposed reconstructs to account for the effects of the being in the exposure chamber. These additional steps, even though they increase the duration of the experiment, need to be taken to ensure that we can accurately compare our exposure scenarios. Also increased sample sizes are needed to improve the statistical power of the study. Due to the low sample size of the pilot study it was difficult to determine the statistical significance of the different exposures. In addition, the increased sample size would allow us to place reconstructs in each well of the 6-well plate. This would allow us to determine if benzene exposure inside the chamber is equal and understand the variability between the reconstructs.

## 5. Conclusions

These initial experiments using our benzene generation and exposure-chamber system validated our ability to deliver a constant concentration of benzene to an *in vitro* exposure chamber. However, we were not able to use the *in vitro* skin and lung reconstructs to quantify our benzene exposures with the current experimental design.

The skin reconstructs were resilient to the benzene exposure at the delivered concentrations, which we attribute to the protective function of the stratum corneum layer. The skin reconstructs had no observable difference from clean-air exposed at any of the three exposure concentrations. The lack of significantly different cytotoxic response between the skin reconstructs is supported by the low permeability of benzene through human skin (McDougal et al. 1990). Despite low permeability, higher concentrations of skin exposures to benzene, for similar exposure duration, have been linked with health effects (Luttrel and Conley, 2011). Thus, future experiments should aim at further defining the exposure concentrations that produce a quantifiable exposure-response in the skin reconstructs.

The week 2 lung reconstructs exhibited a LDH activity significantly different, relative to the unexposed control, once the ability to produce mucous had been diminished over the course of the experiment. However, due to the multiple variables introduced by our experimental design, we cannot attribute the observed cytotoxicity to benzene exposure alone. Clearly defined controls need to be used to account for factors that potentially introduce variability into measured LDH activity such as age, position of reconstruct, mucous production, and exposure chamber conditions (air flow and humidity).

The results from this study indicate that there is a potential for using reconstructs as a model for the biological assessment of toxic effects due to xenobiotic vapor exposure. While the skin reconstructs provided limited insight into the exposure-effect relationship to benzene vapor exposure, the increase in the cytotoxicity and the morphological changes in the lung reconstructs indicate a potential for quantifying an exposure-effect relationship. In order to clearly establish exposure-effect relationship, future studies are warranted to account for all potential variables that can influence the effect outcomes. In addition, multiple exposures need to be tested in order to determine the variability in the exposure-effect relationship between individual samples.

**References**

American Conference of Governmental Industrial Hygienists (ACGIH). (2011) TLVs and BEIs Based on the Documentation of the Threshold Limit Values for Chemical Substances and Physical Agents & Biological Exposure Indices

ATSDR (Agency for Toxic Substances and Disease Registry): Toxicological Profile for Benzene. Division of Toxicology and Environmental Medicine/Applied Toxicology Branch, U.S. Public Health Service, Atlanta, GA (2007).

Bahadar, H., Mostafalou, S., Abdollahi, M. (2014) Current understandings and perspectives on non-cancer health effects of benzene: A global concern. *Toxicology and Applied Pharmacology (In press)*

Balharry, D., Sexton, K., BeruBe, K.A. (2008) An in vitro approach to assess the toxicity of inhaled tobacco smoke components: Nicotine, cadmium, formaldehyde and urethane. *Toxicology 244*, 66-76

Blank, I.H., McAuliffe, D.J. (1985) Penetration of Benzene through Human Skin. *The Journal of Investigative Dermatology 85*, 522-526

Brohem, C.A., da Silva Cardeal, L.B., Tiago, M., Soengas, M.S., de Moreaes Barros, S.B., Maria-Engler, S.S. (2010) Artificial skin in perspective: concepts and applications. *Pigment cell Melanoma Research 24*, 35-50

Bronaugh, R.L., Stewart, R.F., Congdon, E.R. (1982) Methods for in Vitro Percutaneous Absorption Studies II. Animal Models for Human Skin. *Toxicology and Applied Pharmacology 62*, 481-488

Caprette, David R. Colorimetric Assays. Rice University. August 10, 2012. http://www.ruf.rice.edu/~bioslabs/methods/protein/protcurve.html

Cayman Chemical Company. LDH Cytotoxicity Assay Kit. Item No. 10008882. March 5, 2012.

Chilcott, R.T. (2008) Cutaneous Anantomy and Function. In Chilcott, R.T., Price, S., eds. *Principles and Practice of Skin Toxicology*. (3-16). Chichester, UK: John Wiley & Sons, Ltd

Choi, S., Kim, J., Moon, J., Baek, H.J., Seo, S. (2011) Differential Gene Expression Analysis in K562 Human Leukemia Cell Line Treated with Benzene. *Official Journal of Korean Society of Toxicology 27*, 43-48

McHale, C.M., Zhang, L., Smith, M.T. (2011) Current understanding of the mechanism of benzene-induced leukemia in humans: implications for risk assessment. *Carcinogenesis* doi: 10.1093/carcin/bgr297

Clontech Laboratories Inc. LDH Cytotoxicity Detection Kit User Manual. Cat. No. 630117. PT3947-1 (PR6Y2138). January 17, 2007.

Elliot, N.T., Yuan, F. (2010) A Review of Three-Dimensional *In Vitro* Tissue Models for Drug Discovery and Transport Studies. *Journal of Pharmaceutical Sciences 100*, 59-74

Gibbons, M.C., Foley, M.A., MS, Cardinal, K.O. (2013) Thinking Inside the Box: Keeping Tissue-Engineered Constructs *In Vitro* for Use as Preclinical Models. *Tissue Engineering: Part B 19*, 15-30

Gibbs, S., van de Sandt, J.J.M., Merk, H.F., Lockley, D.J., Pendlington, R.U., Pease, C.K. (2007) Xenobiotic Metabolism in Human Skin and 3D Human Skin Reconstructs: A Review. *Current Drug Metabolism 8*, 758-772

Green, M., Seiber, J.N., Biermann, H.W. (1993) In-situ measurements of volatile toxic organics in indoor air using long-path Fourier Transform Infrared Spectroscopy. Proc. SPIE 1716 *International Conference on Monitoring of Toxic Chemicals and Biomarkers 157*,

Gwinn, W.M., Flake, G.P., Bousquet, R.W., Morgan, D.L. Characterization of Diacetyl Vapor-Induced Airway Toxicity Using the Human EpiAirway in Vitro Model. *Respiratory Technology, NTP Laboratories*. Alion Science and Technology Corp. Available: http://www.mattek.com/700-characterization-of-diacetyl-vapor-induced-airway-toxicity-using-the-human-epiairwaytm-in-vitro-model (last accessed 5/6/2014).

Henderson, R.F. (1996) Species Differences in the Metabolism of Benzene. *Environmental Health Perspectives 104*, 1173-1175

Harper M. (2000) Sorbent trapping of volatile organic compounds from air. *Journal of Chromatography A 885*, 129-151

Hu, T., Khambatta, Z.S., Hayden, P.J., Bolmarcich, J., Binder, R.L., Robinson, M.K., Carr, G.J., Tiesman, J.P., Jarrold, B.B., Osborne, R., Reichling, T.D., Nemeth, S.T., Aardema, M.J. (2010) Xenobiotic metabolism gene expression in the EpiDerm™ in vitro 3D human epidermis model compared to human skin. *Toxicology in Vitro 24*, 1450-1463

Krol, S., Zabiegala, B., Namiesnik, J. (2010). Monitoring VOCs in Atmospheric air 1.On-line gas analyzers. *Trends in Analytical Chemistry 29*, 1093-1100

Liu, F.F., Peng, C., Escher, B.I., Fantino, E., Giles, C., Were, S., Duffy, L., Ng, J. C. (2013) Hanging drop: An in vitro air toxic exposure model using human lung cells in 2D and 3D structures. *Journal of Hazardous Materials 261*, 701-710

Luttrell, W.E., Conley, N.L. (2011). Benzene. *Journal of Chemical Health and Safety 18*, 32-33

McDougal J.N. (1991) Dermal Absorption of Neat and Aqueous Volatile Organic Chemicals in the Fischer 344 Rat. *Environmental Research 55*, 51-63

McDougal, J.N., Jepson, G.W., Clewell III, H.J., Andersen, M.E., (1985) Dermal Absorption of Dihalomethane Vapors. *Toxicology and Apllied Pharmacology 79*, 150-158

McDougal, J.N., Jepson, G.W., Clewell III, H.J., Gargas, M.L., Andersen, M.E., (1990) Dermal Absoprtion of Organic Chemical Vapors in Rats and Humans. *Fundamental and Applied Toxicology 14*, 299-308

Midzenski, M.A., McDiarmid, M.A., Rothman, N., Kolodner, K. (1992) Acute High Dose Exposure to Benzene in Shipyard Workers. *American Journal of Industrial Medicine 22*, 553-565

Milchak, L.M., Brandwein, D.H., Zappia, J. (2013)Incorporation of Reconstructed Human Epidermal Tissues Into a Corporate Toxicology Laboratory: Use of in Vitro Test Data for Diverse Safety and Risk Assessment Applications. *Presented at SOT 2013, San Antonio, TX*

Molhave, L., Clausen, G., Berglund, B., De Ceaurriz, J., Kettrup, A., Lindvall, T., Maroni, M., Pickering, A.C., Risse, U., Rothweiler, H., Seifert, B., Younes, M. (1997) Total Volatile Organic Compounds (TVOC) in Indoor Air Quality Investigations. *Indoor Air 7*, 225-240

Morgan, D. L., Cooper S. W., Carlock, D.L., Sykora, J. J., Sutton, B., Mattie D. R. (1991) Dermal absorption of Neat and aqueous volatile organic chamicals in the Fischer 344 rat. *Environmental Research 55*, 51-63

Murphy, C.H. (1991) The USeof Whole Animals Versus Isolated Organs or Cell Culture in Research. *Transactions of the Nebraska Academy of Sciences and Affiliated Societies 18*, 105-108

Murugesan, K., Baumann, S., Wissenbach, D.K., Kliemt, S., Kalkhof, S., Otto, W., Mogel, I., Kohajda, T., von Bergen, M., Tomm, J.M. (2013) Subtoxic and toxic concentrations of benzene and toluene induce Nrf2-mediated antioxidative stress response and affect the central carbon metabolism in lung epithelial cells A549. *Proteomics 13*, 3211-3221

Nelson, G.O. (1971) Controlled Test Atmosphere: Principles and Techniques. Ann Arbor Science Publishers.

NRC. (2007). *Toxicity Testing in the 21st Century: A Vision and a Strategy.* Washington D.C.: The National Academic Press

Pampaloni, F., Reynaud, E.G., Stelzer E.H.K. (2007) The third dimension bridges the gap between cell culture and live tissue. *Nature Reviews Molecular Cell Biology 8*, 839-845

Pariselli, F., Sacco, M.G., Ponti, J., Rembges, D. (2009) Effects of toluene and benzene in air mixtures on human lung cells (A549). *Experimental and Toxicologic Pathology 61*, 381-386

Poet, T.S., McDougal, J.N. (2002) Skin Absorption and human risk assessment. *Chemico-Biological Interactions 140*, 19-34

Rappaport, S.M., Kim, S., Thomas, R., Johnson, B.A., Bois, F.Y., Kupper, L.L. (2013) Low-dose Metabolism of Benzne in Humans: Science and Obfuscation. *Carcinogenesis 34*, 2-9

Rogers, D.F. (1994) Airway goblet cell: responsive and adaptable front-line defenders. *European Respiratory Journal 7*, 1690-1706

Sarma, S.N., Kim, Y., Ryu, J. (2010) *Toxicology 271*, 122-130

Tissupath. TissuPath Specialist Pathology Services. Sept. 2011

Tupker, R. A. (2003) Prediction of irritancy in the human skin irritancy model and occupational setting. *Contact Dermatitis 49*, 61–69

Valentine, J.L., Lee, S.S-T, Seaton, M.J., Asgharian, B., Farris, G., Corton, J.C., Gonzalez, F.J., Medinsky, M.A. (1996) Reduction of Benzene Metabolism and Toxicity in Mice That Lack CYP2E1 Expression. *Toxicology and Applied Pharmacology 141*, 205-213

Weisel, C.P. (2002) Assessing Exposure to Air Toxics Relative to Asthma. *Environmental Health Perspectives 110*, 527-537

Wester, R.C., Maibach, H.I. (2000) Benzene percaneous absorption dermal exposure relative to other benzene sources. *International Journal of Occupational and Environmental Health 6*, 122-126

Wilhelm, K-P., Böttjer, B., Siegers, C-P. (2001) 0. *British Journal of Dermatology 145*, 709-715

Wright, J.L., Cosia, M., Churg. A. (2008) Animal models of chronic obstructive pulmonary disease. *American Journal of Physiology – Lung Cellular and Molecular Physiology 295*, 1-15

Woolfenden, E. (2010) Sorbent-based sampling methods for volatile and semi-volatile organic compounds in air. Part 2. Sorbent selection and other aspects of optimizing air monitoring methods. *Journal of Chromatography A 1217*, 2685-2694

Yin, S.N., Li, G.L.. Tain, Z.I.F., Jin, C., Chen J., Luo, S.J., Ye, P.Z., Zhang, J.Z., Wang, G.C. (1987) Leukaemia in Benzene Workers: a retrospective cohort study. *British Journal of Industrial Medicine 44*, 124-128

Yu, R., Weisel, C.P. (1996) Measurement of benzene in human breath associated with an environmental exposure. *Journal of Exposure Analysis and Environmental Epidemiology 6*, 261-277